Rampart craters on Ganymede: Their implications for fluidized ejecta emplacement

Joseph BOYCE[1*], Nadine BARLOW[2], Peter MOUGINIS-MARK[1], and Sarah STEWART[3]

[1]Hawaii Institute of Geophysics and Planetology, University of Hawaii, Honolulu, Hawaii 96922, USA
[2]Department of Physics and Astronomy, Northern Arizona University, Flagstaff, Arizona 86001, USA
[3]Department of Earth and Planetary Science, Harvard University, Cambridge, Massachusetts 02138, USA
[*]Corresponding author. E-mail: jboyce@higp.hawaii.edu

Abstract–Some fresh impact craters on Ganymede have the overall ejecta morphology similar to Martian double-layer ejecta (DLE), with the exception of the crater Nergal that is most like Martian single layer ejecta (SLE) craters (as is the terrestrial crater Lonar). Similar craters also have been identified on Europa, but no outer ejecta layer has been found on these craters. The morphometry of these craters suggests that the types of layered ejecta craters identified by Barlow et al. (2000) are fundamental. In addition, the mere existence of these craters on Ganymede and Europa suggests that an atmosphere is not required for ejecta fluidization, nor can ejecta fluidization be explained by the flow of dry ejecta. Moreover, the absence of fluidized ejecta on other icy bodies suggests that abundant volatiles in the target also may not be the sole cause of ejecta fluidization. The restriction of these craters to the grooved terrain of Ganymede and the concentration of Martian DLE craters on the northern lowlands suggests that these terrains may share key characteristics that control the development of the ejecta of these craters. In addition, average ejecta mobility (EM) ratios indicate that the ejecta of these bodies are self-similar with crater size, but are systematically smaller on Ganymede and Europa. This may be due to the effects of the abundant ice in the crusts of these satellites that results in increased ejection angle causing ejecta to impact closer to the crater and with lower horizontal velocity.

INTRODUCTION

We have identified layered ejecta craters on Ganymede whose layers terminate in ramparts similar to those of layered ejecta craters on Mars (Figs. 1A and 1B). The morphology of these craters suggests that their ejecta were fluidized during emplacement in a manner similar to Martian layered ejecta. For example, high-resolution images show that the ejecta of these craters flowed around pre-impact obstacles (Fig. 2B) suggesting emplacement as ground-hugging flows similar to Martian fluidized ejecta. These are characteristics that typically have been used as criteria for identifying fluidized ejecta (e.g., Carr et al. 1977; Horner and Greeley 1982). Pedestal craters (i.e., craters surrounded by a platform elevated well above the surrounding terrain, usually attributed to differential erosion) have been identified on Europa (Moore et al. 2001) and

Dione (Jaumann et al. 2009); some of the pedestal craters on Europa appear to also terminate in rampart ridges (Fig. 1C). There is also evidence that the continuous ejecta deposit of the fresh terrestrial fluidized ejecta crater Lonar also may terminate in a rampart (Maloof et al. 2009). The morphology of all of these craters suggests that they are fluidized ejecta craters. Collectively they have implications for models of emplacement of fluidized ejecta and, most importantly, the role of volatiles in the fluidization process.

Historically, it has been assumed that volatiles must be involved in facilitating the flow of ejecta on Mars, but the exact role played by volatiles and the source of these volatiles for fluidization are still major unresolved issues. Most current models for ejecta fluidization propose that the volatiles were derived either from (1) the target materials (e.g., Carr et al. 1977; Gault and

Ganymede   **Europa**
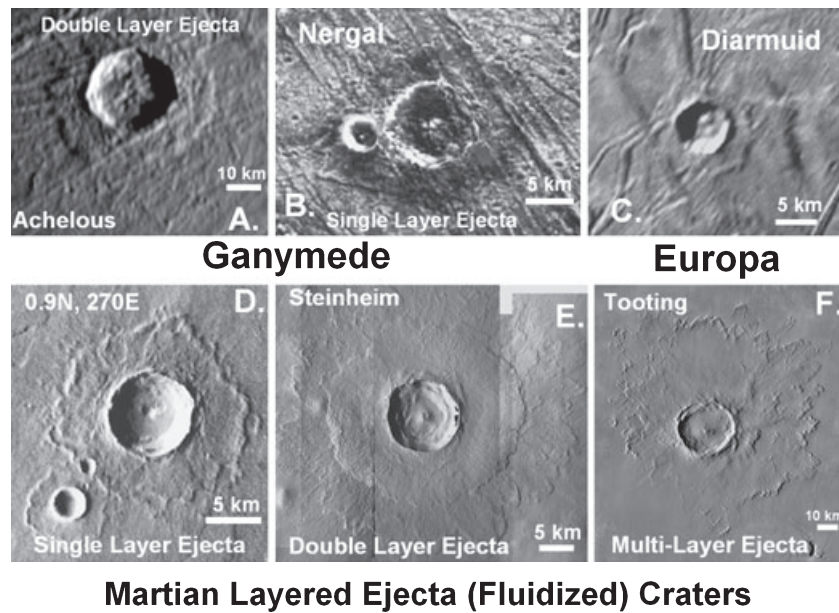
Martian Layered Ejecta (Fluidized) Craters

Fig. 1. Examples of rampart layered ejecta craters on Ganymede, Europa, and Mars. A) The approximately 35 km diameter Ganymede double-layer ejecta crater (DLE) Achelous (Galileo image, PIA 01660 NASA/JPL/DLR). B) The approximately 8 km diameter Ganymede single-layer ejecta (SLE) crater Nergal (Galileo Image PI 01088). (C) The approximately 7.8 km diameter crater on Europa, Diarmuid (Galileo image s0466676914.2). The Martian craters include, on the left, i.e., (D) the unnamed 8.1 km diameter SLE crater located at 0.9N, 270.4E, the crater in the center (E) is the 10 km diameter DLE crater Steinheim, and the crater on the right (F) is the 29.7 km diameter multilayer ejecta crater Tooting. D: THEMIS VIS images V18626001; E: mosaic containing THEMIS Images V05199007, V19926001, V21199003, V20213002; and F: ASU THEMIS mosaic, respectively.
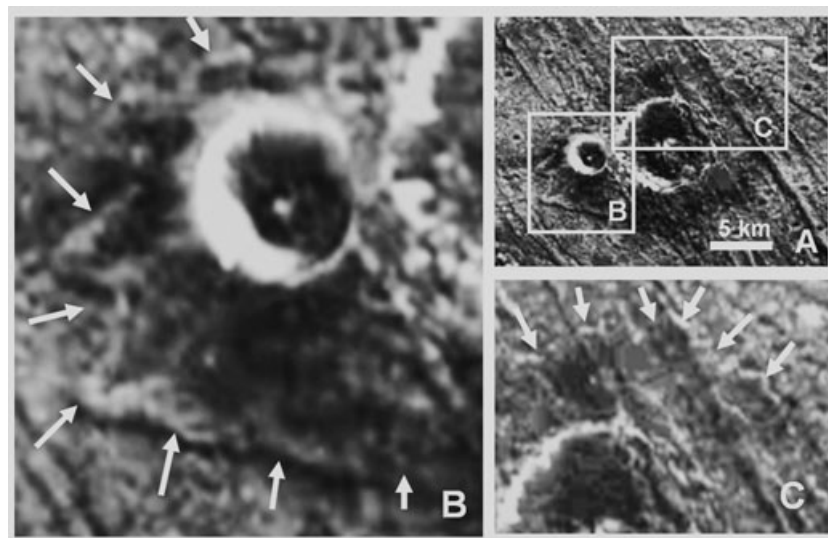

Fig. 2. Nergal crater (A) is an approximately 8 km SLE diameter crater on Ganymede. Its continuous ejecta blanket appears to have only a single layer that terminates in a rampart ridge (enlarged in B and C). The arrows show the location of the rampart. The lack of substantial ejecta from Nergal or the small crater on its left in the other's interior suggests that, like for Martian fluidized ejecta craters, the ejecta was most likely transported as a ground-hugging flow (Galileo Image PIA01088, NASA/JPL/Brown University, resolution approximately 86 m per pixel).

Greeley 1978; Mouginis-Mark 1978, 1979; Wohletz and Sheridan 1983; Boyce and Mouginis-Mark, 2006; Osinski 2006; Senft and Stewart 2008), (2) the atmosphere (e.g., Schultz and Gault 1979; Schultz 1992; Barnouin-Jha and Schultz 1996, 1998; Barnouin-Jha et al. 1999), or (3) some combination of both (Barlow
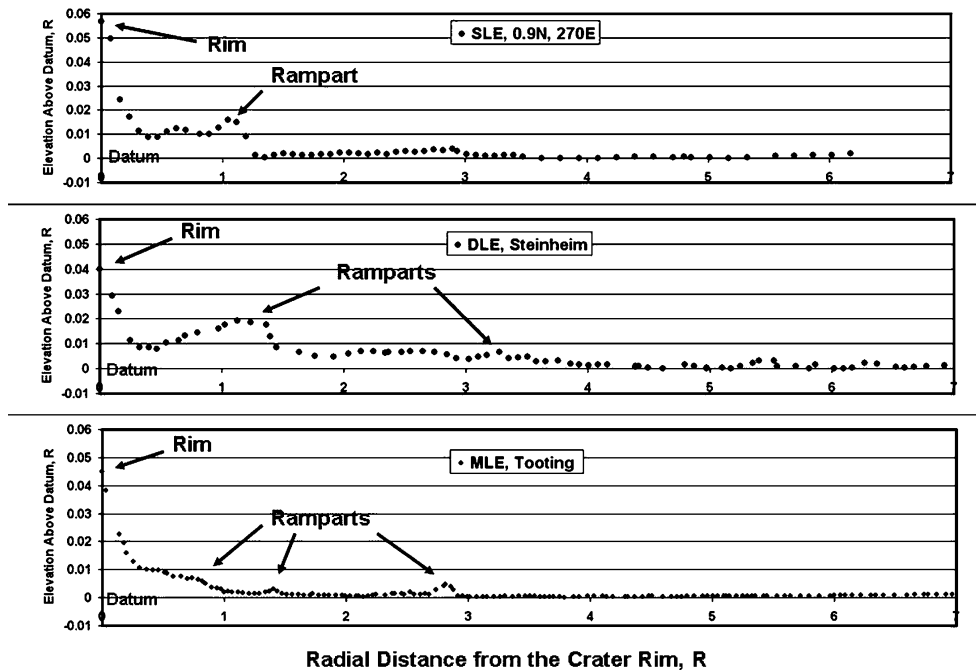
Fig. 3. Topographic profiles (normalized to crater radius) of the three major types of Martian layered ejecta craters (craters D, E, and F in Fig. 1). The individual points are MOLA shot data (individual points are shots) along ground tracks that passed closest to the center of the craters. In addition, these profiles were constructed by averaging MOLA shot data on each side of the crater so that they represent a more generalized geometry. The distribution of ejecta mass is different from crater type to crater type, with the inner layer of DLE craters being proportionally much wider and higher that the ramparts of its outer layer or the ramparts of SLE and MLE layered ejecta craters.

2005a, 2005b; Komatsu et al. 2007). It also has been suggested that ejecta flow could be the result of dry granular flow (i.e., Barnouin-Jha et al. 2005; Wada and Barnouin-Jha 2006). Laboratory experimental studies with dry granular materials have shown that some Martian mass movements have morphologies consistent with emplacement through dry granular flow processes (Shinbrot et al. 2004).

Martian fluidized ejecta show features suggesting that after ballistic ejection from the crater, these materials moved across the surface as a ground-hugging flow (e.g., see Carr et al. 1977; Gault and Greeley 1978; Schultz and Gault 1979; Horner and Greeley 1982; Schultz 1992; Baloga et al. 2005; Baratoux et al. 2005; Osinski 2006; Mouginis-Mark and Garbeil 2007). On Mars, the resultant ejecta are generally characterized by broad, thin, ejecta deposits that terminate in a lobate, convex, marginal ridge, or rampart (Figs. 1D–F and 3). These deposits may include one or more ramparts that formed at increasing distance from the rims. This gives the appearance of layering of the ejecta deposits, but it may not be due to a succession of superposed layers at all. Instead, it may be due to instabilities that develop within the flowing ejecta that produce such phenomena as surging like that observed in debris and ash flows

(e.g., Wohletz and Sheridan 1983; Major and Iverson 1999). A variety of names has been applied to these craters, for example: fluidized ejecta craters, layered-ejecta craters, rampart craters, and flower craters. Here, we adopt the convention proposed by Barlow et al. (2000) and use "layered ejecta craters" with the modifier: rampart. In addition, we will refer to the Ganymede rampart layered ejecta craters or GRLE craters here.

The GRLE craters and the pedestal craters on Europa may provide some tantalizing insights into the ejecta fluidization controversy because they occur in environments that are markedly different than the terrestrial planets. Previous studies have described elevated lobate, layered ejecta deposits on Ganymede, attributing their morphology to the effects of volatiles in the target (e.g., Lucchitta 1980; Strom et al. 1981; Horner and Greeley 1982; Moore et al. 1998). However, none of these studies recognized the existence of the population of layered ejecta craters that include one of the most diagnostic features considered indicative of ground-hugging flow: distal ramparts. This is most likely because either the studies were carried out before readily available PC-based image processing capabilities were available to bring out the ramparts on the images,

or the goals of the studies were not specifically aimed toward this issue.

In addition, the ejecta of some Earth craters, such as Ries and Lonar craters, show evidence for ejecta fluidization and may provide additional insight into the issue of ejecta fluidization (e.g., Pohl et al. 1977; Hörz et al. 1983; Osinski et al. 1987; Kenkman and Schonian 2005; Osinski 2006; Maloof et al. 2009). Recently, Maloof et al. (2009) have studied the crater Lonar in India and suggest that it may have the remnants of an eroded ejecta rampart. This is a valuable observation because it provides an example of ejecta fluidization on a rocky planet with a relatively strong gravity field, abundant liquid water, and a substantial atmosphere. However, the small size of Lonar crater may mean that it formed in the strength controlled regime, and hence caution should be taken in comparing it with larger craters on other planets.

In contrast with layered ejecta, impact craters on the bodies mentioned here, impact craters on other solar system bodies, including other icy satellites, exhibit ejecta morphologies that suggest, at best, only limited ejecta flow has occurred during initial emplacement (Smith et al. 1979a, 1979b; Pike 1980, 1988; Horner and Greeley 1982; Schenk 1991; Schultz 1992; Alexopoulos and McKinnon 1994; Herrick et al. 1997; Barnouin-Jha and Schultz 1998; Moore et al. 1998; Moore et al. 2004; Elachi et al. 2006; Jaumann et al. 2009) (note: Venus is a special case that does not apply here and Dione has several pedestal craters that appear to lack ramparts). Hence, the unique nature of ejecta on Ganymede, Europa, Mars, and Earth, their distinctly different geology and surface environments from one another, and the absence of fluidized ejecta craters formed in a broad spectrum of environments on other solar system bodies place important constraints on models of ejecta fluidization and its causes.

Background

Lucchitta (1980) and Strom et al. (1981) first reported fresh impact craters on Ganymede with relatively flat, elevated ejecta blankets that terminate in a sharp, scarp-like outer edge. Horner and Greeley (1982) called these craters "pedestal craters" (GRLE are a subset of these craters) because their raised ejecta platform resembles those of Martian pedestal craters. Horner and Greeley (1982) suggested that, because Ganymede lacks an atmosphere, these craters may provide information about the degree to which an atmosphere contributes to the ejecta morphologies on Mars. However, based on the available relatively low-resolution Voyager images, Horner and Greeley (1982) were unable to identify morphologic features suggestive of flow similar to those of Martian crater ejecta (e.g., the presence of flow structure on ejecta surfaces such as ramparts, and the existence of thin outer flow lobes seen around Martian multilayered craters). They also noted that the ratio of ejecta diameter to crater diameter (i.e., ejecta mobility or EM) was relatively low, similar to the inner ejecta layer of some Mars craters and the continuous ejecta of lunar craters. They suggested that this might be due to the steepness of the ejecta angles caused by impact into volatile targets like Ganymede, as had been suggested by Greeley et al. (1980). In mapping the locations of these craters, Horner and Greeley (1982) also found that pedestal craters appeared to be located only in the grooved terrain. They attributed this distribution to the difficulty in identification due to the low-albedo, rugged topography of the dark terrain, and not a paucity of pedestal craters in that terrain.

Moore et al. (1998), using higher-resolution (up to approximately 87 m per pixel) Galileo data, found that some pedestal craters on Ganymede also include an outer ejecta layer (one of Horner and Greeley's criteria for evidence of flow). In addition, they noted that some of the freshest of these craters show hummocky, dune-like flow features similar to those found in lunar crater ejecta (Gault et al. 1968; Oberbeck 1975). They attributed the morphology of the pedestal facies of the ejecta on both Europa and Ganymede to thermal creep (i.e., instead of being primary ejecta morphology, the rampart formed by gravity-driven creep that resulted in relief flattening movement of plastically deforming but otherwise solid ice that warmed at the time of emplacement). But this explanation requires that topography at the outer edge of the pedestal behaves rheologically differently than other parts of the pedestal, as well as for the stress necessary to lift the rampart to be transferred a few kilometers in slowly flowing ice.

Neal and Barlow (2003) and Barlow (2005b) used both Voyager and Galileo image data to investigate the geometry of the shapes of craters on Ganymede. They found that (about 4%) of the pedestal craters are double-layered ejecta craters. In addition, they measured the ejecta mobility (EM) ratio for continuous ejecta, where

$$EM = \frac{(\text{maximum ejecta extent measured from crater rim})}{(\text{crater radius})} \quad (1)$$

and the lobateness of the outer ejecta perimeter of the ejecta (i.e., sinuosity) (Γ)

$$\Gamma = \frac{(\text{ejecta perimeter})}{(4\pi(\text{ejecta area}))^{1/2}} \quad (2)$$

of pedestal craters on Ganymede. Neal and Barlow (2003) and Barlow (2005b) compared these parameters

with those of the layered ejecta of Martian crater ejecta and found general similarities. They also found the EM values of both single and double-layered ejecta craters on Ganymede are lower than their counterparts on Mars. Moreover, Neal and Barlow (2003) and Barlow (2005b) suggest that Γ values of Ganymede craters are near 1.0 and vary little with crater size compared with Martian craters, which vary from 1.0 to 6.4. They attributed the differences in these values to the effects of colder and purer ice crust on Ganymede compared with that of Mars.

We will describe the morphometric characteristics of GRLE craters as well as crater ejecta on Europa and Mars in the next section. In the Discussion section, we will discuss the implications of these morphometric traits to likely ejecta fluidization processes, as well as the possible influence of environmental conditions on such fluidization.

EJECTA MORPHOLOGY AND MORPHOMETRY

A key to understand the mode of emplacement of fluidized ejecta is the geometry of fluidized ejecta deposits because, to first order, the shape of a geomorphic feature is a reflection of the processes that produced it (e.g., Hack 1960; Wilson 1968; Ritter et al. 2002). However, the scarcity of high-resolution image coverage and lack of topographic information restrict the types of morphometric measurements that can be collected for GRLE and Europa crater ejecta. Even with this limitation, there are some planimetric measurements of large-scale features that can be collected that may shed light on the flow properties of the ejecta during emplacement. In particular, EM and Γ have been measured for crater ejecta on Ganymede (Horner and Greeley 1982; Neal and Barlow 2003, 2004; Barlow 2005a, 2005b), and of Mars layered ejecta (Barlow 2005a, 2005b, 2006a, 2006b). These attributes are thought to be controlled by the rheological properties of the ejecta, and hence provide information about the physical nature of the ejecta and the flow process (e.g., Carr et al. 1977; Gault and Greeley 1978; Mouginis-Mark 1978, 1979, 1981; Schultz and Gault 1979; Horner and Greeley 1982; Costard 1989; Kargel 1989; Schultz 1992; Neal and Barlow 2003, 2004; Baloga et al. 2005; Baratoux et al. 2005; Barlow 2005a, 2006a).

We have collected morphometric and other data of craters that exhibit continuous ejecta deposits that terminate in rampart ridges on Ganymede, Europa, Mars, and Earth. For Ganymede and Europa image data, we have applied simple contrast enhancement (giving careful attention to image processing edge effects that can produce rampart-looking edge features) to

Voyager and Galileo high-resolution images to identify these craters and to allow measurement of the geometry of their ejecta blankets. Most measurements of Martian ejecta were made using THEMIS VIS and MOLA shaded relief images.

Resolution of the Ganymede images used in this analysis range from about 0.086 km per pixel for the smallest crater to approximately 1.5 km per pixel for the largest craters studied and were taken at relatively low-sun angle (< approximately 15°). We have identified 26 GRLE craters on Ganymede (Table 1) and six fresh pedestal craters on Europa (Table 2) that may be fluidized ejecta craters (Fig. 1). Other craters on both satellites may be layered ejecta craters, but low image quality or the degree of degradation of these craters reduce our confidence in their identification as such craters, and hence these are not included in this study. GRLE craters identified in this study range in diameter from approximately 8 km to 115 km and are most readily identified in the highest resolution images (> approximately 1.0 km per pixel) taken at sun angles of < approximately 10°. Europa layered ejecta craters range in size from 7.9 km to 28.4 km diameter and are the freshest of those identified by Moore et al. (2001). Martian craters used in this study range from 7.0 km to 55.2 km in diameter. These craters were chosen because they have fresh appearing morphologies (i.e., their small-scale primary features such as secondary craters are preserved) with well-preserved ramparts, have relatively symmetrical ejecta blankets, and are located in different geographic and geologic regions. In addition, morphometric and geologic data for the fresh 1.9 km diameter terrestrial crater Lonar was recently collected by Maloof et al. (2009). These data also will be used in this study and are listed in Table 2.

GRLE craters are found exclusively on the grooved terrain and over a broad latitude range (from 82°N to −78°S), consistent with the findings of Horner and Greeley (1982). Morphologically fresh craters also are common in the dark heavily cratered terrain, but we have not identified ramparts associated with any of these craters.

Most GRLE craters appear to have pedestal-like ejecta deposits with only a single ejecta layer, but these may be the inner ejecta layer of double-layer ejecta (DLE) craters. Nearly one-fourth of GRLE craters identified exhibit a relatively thin, lobate, outer ejecta layer that also terminates in a rampart (Fig. 4). Outer ejecta layers such as these may be more common, but because these features are relatively low-relief, and because of the limited availability of high quality image data, these features can be difficult to resolve.

However, some GRLE craters appear to be single-layered ejecta (SLE craters with only one ejecta layer).

Table 1. Rampart width and ejecta mobility data of ejecta layers of fresh GRLE craters measured for this study.

Crater name	Approx. long.	Approx. lat.	Crater dia., km	GRLE inner layer, wav, km	GRLE outer layer, wav, km	GRLE inner layer, wav, ratio	GRLE outer layer, wav, ratio	GRLE inner layer, EM, km	GRLE outer layer, EM, km	GRLE inner layer, EM, ratio	GRLE outer layer, EM, ratio
1. Nergal	201.0	39.0	8	0.8		0.2		4		1	
2. Unnamed	310.0	8.0	20	4.9		0.5		7.5		0.8	
3. Unnamed	250.0	−77.0	20	5.7		0.6					
4. Unnamed	345.0	64.0	23	5.6		0.5		8.2		0.7	
5. Unnamed	122.0	−33.0	31	4.1		0.3		11.8		0.8	
6. Unnamed	182.0	52.0	25	5.6		0.4		9.4		0.8	
7. Unnamed	156.0	−73.0	25	6		0.5		11.8		0.9	
8. Unnamed	130	−4	28	6.5		0.5		11.7		0.8	
9. Enlil	48	54	43	10.3		0.5		17.4		0.8	
10. Unnamed	254	−78	30	6		0.4		12.2		0.8	
11. Unnamed	340	85	30	8.4		0.6		14		0.9	
12. Unnamed	29	70	30	8.6		0.6		15.8		1.1	
13. Unnamed	35	70	30	7.9		0.5		13.3		0.9	
14. Unnamed	310	−20	25	7.2		0.6		11.1		0.9	
15. Unnamed	10	82	32	5.2		0.3		10.9		0.7	
16. Unnamed	253	−78	35	8.8		0.5		14.3		0.8	
17. Achelious	12	62	35	8.2	2.45	0.5	0.14	15.6	35	0.9	2
18. Unnamed	312	−4	37	7.7		0.4		12.1		0.7	
19. Gula	13	64	40	9		0.4		18.5		0.9	
20. Etana	341	75	49	10.9		0.4		18.7		0.8	
21. Andijeti	161	−53	65	7.6	3.5	0.2	0.11	27.7		0.9	
22. Unnamed	56	−15	50	8		0.3					
23. Sebek	357	61	67	9.3	4.47	0.3	0.13	30.2	63.7	0.9	1.9
24. Ashima	123	−39	82	9.8	4.1	0.2	0.1	28.7	69.7	0.7	1.7
25. Ta-urt	304	27	85	16.3	5.1	0.4	0.12	29.8	76.5	0.7	1.8
26. Irkalla	115	−32	116	18.3	5.22	0.3	0.09	40.6	98.6	0.7	1.7

Table 2. Rampart width and ejecta mobility data of ejecta layers of fresh Europa pedestal craters measured for this study.

Crater name	Approx. lat.	Approx. long	Crater dia.	Wav, km	Wav ratio	EM km	EM ratio	Γ
Diarmuid	−61	97	7.9	1.14	0.29	3.4	0.86	1.06
Grainne	−60	95	13.5	1.7	0.25	6	0.89	1.13
Rhiannon	−81	197	15.4			5.6	0.73	
Amerigin	−14.2	230	18.6			6.5	0.7	
Maeve	58.7	75	20.4			7.5	0.74	1.14
Tegid	0.5	164	28.4			13.5	0.95	1.17
Lonar (Earth)	*22.1*	*65.8*	*1.88*	*0.3*	*0.31*	*2.2*	*2.34*	

Data for the terrestrial crater Lonar crater is also included.

For example, the approximately 86 m per pixel image of Nergal crater (Fig. 2A) should be of high enough resolution and low enough sun-angle to show an outer ejecta layer if present, but no such layer is visible. Unlike the pedestal-like inner (or possible only) layer of most GRLE craters, Nergal's continuous ejecta deposit appears to be relatively thin, judging by the modest depth its ejecta buries the small crater located within its ejecta blanket (but enough to obscure the small crater's ejecta blanket). Moreover, considering their close proximity and the lack of appreciable ejecta from Nergal in this small crater, the ejecta from Nergal appears to have been emplaced mainly as a surface flow, similar to fluidized ejecta on Mars. Nergal's rampart also is relatively narrow, similar to those of SLE craters.

Surfaces of GRLE crater ejecta deposits are hummocky at the scale of the highest resolution images
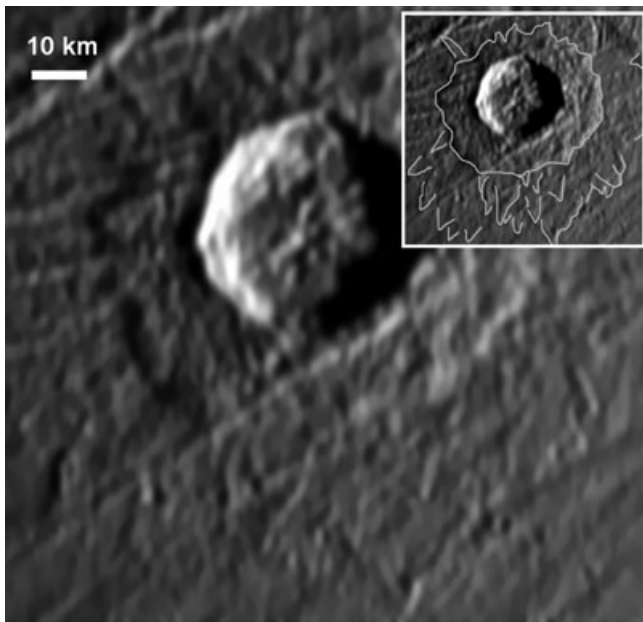
Fig. 4. This composite Galileo image shows a high-resolution (approximately 175 m per pixel) view of the approximately 35 km diameter fresh Ganymede crater Achelous. The inset in the upper right corner shows the location of the lobate edge of the outer ejecta layer marked with white lines. (Galileo image, PIA01660 NASA/JPL/DLR).

(Figs. 2 and 4), but with no hint of the small-scale features common on the Martian crater ejecta blankets, such as the radial grooves of DLE craters (Fig. 2) or the transverse wave-like patterns of troughs and ridges associated with single-layer ejecta (SLE) and multilayer ejecta (MLE) craters (Baloga and Bruno 2005; Boyce and Mouginis-Mark 2006). These Martian features have been attributed to the ejecta flow process and are similar to those found on landslides and debris flows (Baloga et al. 2005; Barnouin-Jha et al. 2005; Boyce and Mouginis-Mark 2006, 2008). Such features are typically a few tens to a few hundred meters across for craters in the size range of most GRLE craters identified here (Boyce and Mouginis-Mark 2006, 2008) and may have not been identified on GRLE crater ejecta because of inadequate image resolution.

The six Europa craters in this study are fresh appearing pedestal craters (Fig. 1), although only two (Grainne and Diarmuid) have obvious terminal ramparts. Neither Grainne nor Diarmuid displays an outer ejecta layer. This may be a result of the lack of images of sufficient quality to identify thin outer ejecta layers at the scale expected for craters of these sizes rather than the ejecta layers being absent. The other four freshest craters display ejecta deposits that are least affected by cross-cutting structural features and terminate in steep terminal cliffs. These observations

indicate that the ejecta deposits are primary features rather than erosional features.

To extend the previous morphometric analyses mentioned earlier, we have also measured average rampart width (W_{av}) as well as the average EM and Γ (for only one GRLE crater) for craters in this study. This has been done for the 26 GRLE (Table 1) and six Europa pedestal (Table 2) craters identified. In addition, we supplemented previous Mars data with similar measurements for 97 (20 SLE, 41 DLE, and 36 MLE) Martian layered ejecta craters (Table 3). While the GRLE craters are found only in the grooved terrain of Ganymede, the Martian craters used in this study are distributed throughout the midlatitudes of Mars on a variety of terrain types (see Table 3 for locations), and were selected because they are the freshest Martian craters with clearly defined ejecta blankets.

We have estimated the approximate measurement error of crater ejecta ramparts W_{av} values used in this study in order to assess the reliability of our measurements and their interpretations. We use the size (in meters) of 2 pixel pairs, i.e., 4 pixels (a pixel pair on each side of the rampart), compared with the measured width of the rampart (in meters) as the method for calculating measurement error. The resulting error is < approximately 20% for the narrowest rampart, using Voyager and Galileo image data for GRLE and Europa ramparts.

Such an estimate is more complicated for Martian ejecta ramparts because of the different slopes on the flanks of the ramparts of different crater types, and the necessity to use more than one type of data for their measurement. For example, the ramparts of Martian SLE, MLE, and outer layer of DLE are relatively narrow (< approximately 0.6 km wide) and have edges that are relatively steep (Mouginis-Mark and Garbeil 2007). The approximately 18 m per pixel resolution of THEMIS VIS images allows the ramparts to be measured to an accuracy of < approximately 12%. In contrast with these narrow, relatively steep-sloped ramparts, DLE inner ejecta layer ramparts are broad features with long, gentle slopes (Boyce and Mouginis-Mark 2006; Mouginis-Mark and Garbeil 2007). The gentleness of the DLE inner layer ramparts slopes produce only limited shading contrast on THEMIS images, and hence our confidence is lowered in places where the rampart begins and ends. However, such low slopes are much more obvious in topographic data and, to a degree, in THEMIS thermal IR data (approximately 100 m resolution). Consequently, our measurements for the broadest of the DLE inner ejecta layer ramparts are based primarily on topographic data. The expected measurement error is < approximately 30% using MOLA data, considering the data set

Table 3. Rampart width and ejecta mobility data of ejecta layers of fresh Martian rampart craters measured for this study.

Crater type	Long.	Lat.	Crater dia. km	Wav: inner, km	Wav: outer km	Wav ratio inner layer	Wav ratio outer layer	EM km inner layer	EM km outer layer	EM ratio inner layer	EM ratio outer layer
DLE	117.3	43.4	39.30	9.0		0.5		21.4	52.1	1.1	2.7
DLE	120.3	40.4	34.00	9.0		0.5					
DLE	136	59.8	29.00	8.0	1.6	0.6	0.11				
DLE	115.6	43	28.20	8.2		0.6		20.1	52.5	1.4	3.7
DLE	139.5	54.3	27.70	8.3	1.7	0.6	0.12	16.1	58.0	1.2	4.2
DLE	118.8	48.9	26.30	7.6		0.6		16.3	36.5	1.2	2.8
DLE	140	55.6	25.80	7.3	1.8	0.6	0.14	13.0	35.7	1.0	2.8
DLE	116.3	39.1	23.40	7.5		0.6		18.2	35.5	1.6	3.0
DLE	118.6	32.9	21.40	6.9	1.6	0.6	0.15	14.9	33.2	1.4	3.1
DLE	133.2	55	20.30	6.5		0.6		16.0	30.4	1.6	3.0
DLE	145.8	48.9	19.60	6.3	1.3	0.6	0.13	16.1	30.4	1.6	3.1
DLE	99.2	38.5	18.50	6.6		0.7		14.8	35.2	1.6	3.8
DLE	101.7	44	16.50	6.5		0.8		13.5	32.0	1.6	3.9
DLE	101.4	35.9	16.20	5.4		0.7		11.7	27.6	1.4	3.4
DLE	120.9	26.7	15.80	4.2	1.2	0.5	0.15	11.8	24.8	1.5	3.1
DLE	101.5	53.2	15.70	4.6		0.6		8.3	25.1	1.1	3.2
DLE	104.1	54.8	15.70	4.0		0.5		9.5	27.4	1.2	3.5
DLE	118	50.3	15.10	4.5		0.6					
DLE	134.5	50.4	14.60	6.1		0.8		11.3	22.7	1.5	3.1
DLE	116.8	58.5	14.60	5.3		0.7		11.5	27.0	1.6	3.7
DLE	98.3	40.9	14.20	5.5		0.8		11.2	23.3	1.6	3.3
DLE	98.2	42.2	14.20	5.5		0.8		9.7	28.1	1.4	4.0
DLE	101.4	33.9	13.90	3.8		0.5		10.5	24.6	1.5	3.5
DLE	102.6	34.9	13.60	4.5		0.7		10.2	23.8	1.5	3.5
DLE	120.5	34.7	13.20	5.0	1.1	0.8	0.17				
DLE	106	54.4	12.60	3.6		0.6					
DLE	49.9	−7.4	12.10	3.4		0.6					
DLE	282.7	23.6	12.10	4.7	0.9	0.8	0.15				
DLE	145	48.9	11.60	3.2	1.1	0.6	0.19				
DLE	147.4	50.1	11.60	4.2	1.1	0.7	0.19	9.2	18.4	1.6	3.2
DLE	105.4	39.5	11.40	5.1		0.9		8.6	19.2	1.5	3.4
DLE	109.6	34.2	10.70	3.2		0.6		8.0	20.0	1.5	3.7
DLE	272.3	−27.7	10.60	3.5	0.9	0.7	0.17				
DLE	103.1	38	10.40	4.1		0.8		4.2	14.7	0.8	2.8
DLE	116.5	29.7	10.40	4.1		0.8		6.8	15.0	1.3	2.9
DLE	277.9	−18.3	10.00	2.9	1.6	0.6	0.32				
DLE	102.3	31.1	9.70	3.7		0.8		7.8	15.5	1.6	3.2
DLE	95.7	56.9	9.70	2.6	0.9	0.5	0.19	8.0	15.0	1.6	3.1
DLE	107.7	36.4	9.50	3.3		0.7		8.0	16.0	1.7	3.4
DLE	112.4	58.7	10	3.6		0.7		6.4	11.2	1.3	2.2
MLE	288.5	10	8.80	0.6	0.6	0.14	0.14	3.9	7.5	0.9	1.7
MLE	287.9	7.2	19.25	1.0	0.9	0.10	0.09	10.9	20.6	1.1	2.1
MLE	287.7	10.4	19.50	0.9	1	0.09	0.10	10.9	20.9	1.1	2.1
MLE	287.7	7.9	19.40	0.8	1.1	0.08	0.11	10.9	18.0	1.1	1.9
MLE	285.3	−20.9	17.80	0.5	1.2	0.06	0.13	6.5	21.0	0.7	2.4
MLE	281.4	−23.1	28.70	1.1	1.5	0.08	0.10	19.4	41.3	1.4	2.9
MLE	279.2	−12.3	19.50	0.8	1	0.08	0.10	11.6	21.3	1.2	2.2
MLE	279.2	−12.3	18.20	0.9	1	0.10	0.11	12.9	22.5	1.4	2.5
MLE	278.6	−11.1	14.40	0.9	1.2	0.13	0.17	9.0	15.5	1.3	2.2
MLE	278.5	−10.1	14.40	0.7	1	0.10	0.14		12.9		1.8
MLE	277.8	−16.1	21.30	1.0	1.3	0.09	0.12	15.5	25.8	1.5	2.4
MLE	275.2	−15.8	18.40	1.1	1	0.12	0.11	15.5	23.2	1.7	2.5

Table 3. *Continued.* Rampart width and ejecta mobility data of ejecta layers of fresh Martian rampart craters measured for this study.

Crater type	Long.	Lat.	Crater dia. km	Wav: inner, km	Wav: outer km	Wav ratio inner layer	Wav ratio outer layer	EM km inner layer	EM km outer layer	EM ratio inner layer	EM ratio outer layer
MLE	273.6	−8.9	13.00	0.9	1	0.14	0.15	7.1	12.5	1.1	1.9
MLE	271.7	−9.6	11.00	0.8	0.9	0.15	0.16	6.5		1.2	
MLE	270.3	−2.5	18.00	0.9	1	0.10	0.11				
MLE	207.8	23.2	26.30	0.9	1.6	0.07	0.12	16.7	38.3	1.3	2.9
MLE	207	28.7	24.50	1.1	1.2	0.09	0.10	13.0		1.1	
MLE	200.3	13.7	22.10	1.0	1.4	0.09	0.13	18.0	30.9	1.6	2.8
MLE	192.9	10.6	29.00	1.1	1.4	0.08	0.10	19.3	39.0	1.3	2.7
MLE	183.2	1	33.50	1.3	1.5	0.08	0.09	21.9	41.9	1.3	2.5
MLE	119.9	28.7	9.90	0.9	0.8	0.18	0.16	5.3	12.6	1.1	2.5
MLE	118.5	23.4	9.50	0.8	0.7	0.17	0.15	5.6		1.2	
MLE	116.8	24.2	10.80	0.8	0.8	0.15	0.15	7.3	12.0	1.4	2.2
MLE	111	17.6	23.80	1.3	1.4	0.11	0.12	16.4	28.9	1.4	2.4
MLE	49.6	−8.8	14.90	0.8	1.3	0.11	0.17		13.8		1.9
MLE	46.5	−0.9	27.20	1.0	1.3	0.07	0.10		21.1		1.6
MLE	41.5	−1.8	17.40	0.9	0.8	0.10	0.09	6.1	23.8	0.7	2.7
MLE	37.3	−11.9	15.60	1.1	0.8	0.14	0.10	9.2	14.9	1.2	1.9
MLE	25.7	−17.1	15.80	1.0	0.9	0.13	0.11	10.6	13.3	1.3	1.7
MLE	23.5	−14.9	16.00	0.7	0.8	0.09	0.10	9.8	20.9	1.2	2.6
MLE	17.9	−13.1	33.10	1.1	1.3	0.07	0.08	20.7	34.2	1.3	2.1
MLE	289	10	10.10	0.7	0.7	0.14	0.14	4.5	8.5	0.9	1.7
MLE	289	9.2	19.50	1.3	1.1	0.13	0.11	14.4	25.5	1.5	2.6
MLE	327	7.5	55.20	2.8	2.8	0.10	0.10				
MLE	290.7	−18.5	22.60	0.8	1.2	0.07	0.11	13.8	2.5	1.2	2.0
MLE	288.8	9.5	13.11	0.9	1.1	0.14	0.17	7.3	12.5	1.1	1.9
SLE	288.5	4.7	12.20	1.1		0.18		6.5		1.1	
SLE	282.9	−19.5	21.00	1.4		0.13		14.8		1.4	
SLE	280.3	−16.9	10.80	0.8		0.15		5.7		1.1	
SLE	279.4	−9.8	10.40	0.9		0.17		12.2		2.3	
SLE	277.8	−17.6	9.50	1.0		0.21		6.3		1.3	
SLE	277	−19.5	10.60	0.9		0.17		5.1		1.0	
SLE	274.8	1.6	13.90	1.1		0.16		8.2		1.2	
SLE	195.4	20.5	13.11	1.0		0.15		7.7		1.2	
SLE	195.2	10.7	7.00	0.8		0.23		3.2		0.9	
SLE	194.4	9	8.10	0.8		0.20		4.5		1.1	
SLE	184.2	21.6	15.10	1.1		0.15		11.6		1.5	
SLE	50.2	−8.7	10.00	1.0		0.20		5.6		1.1	
SLE	49.2	−8.4	15.30	1.1		0.14		9.0		1.2	
SLE	41.5	−18.2	11.00	1.0		0.18		7.2		1.3	
SLE	40.7	−4.6	12.70	1.1		0.17		8.4		1.3	
SLE	34.9	−8.2	12.00	1.1		0.18		7.1		1.2	
SLE	26.5	−13.3	15.50	1.2		0.15		13.5		1.7	
SLE	26	−15.9	14.30	1.2		0.17		7.6		1.1	
SLE	21	−8.2	11.30	1.1		0.19		6.1		1.1	
SLE	1.4	−3.9	12.20	1.1		0.18		7.8		1.3	

resolution (MOLA shot data has a spacing of approximately 300–400 m and the size of the surface feature (the narrowest DLE inner rampart approximately 2.6 km across). We have compared the data on the inner ejecta layers of 16 DLE craters where the interior slopes are steep enough to measure by different techniques and find an average difference of approximately <10% in the measurement of W_{av}. Hence, for these DLE craters the measurement error is approximately 10% for the W_{av} of their inner ejecta
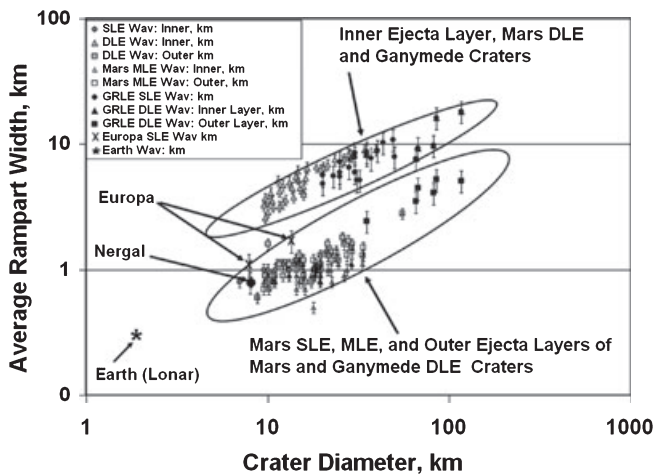
Fig. 5. This plot shows that the ramparts fall into two major groups that widen with increased crater size. Ellipses enclose members of each parameter and are not meant to define limits beyond where data exists.
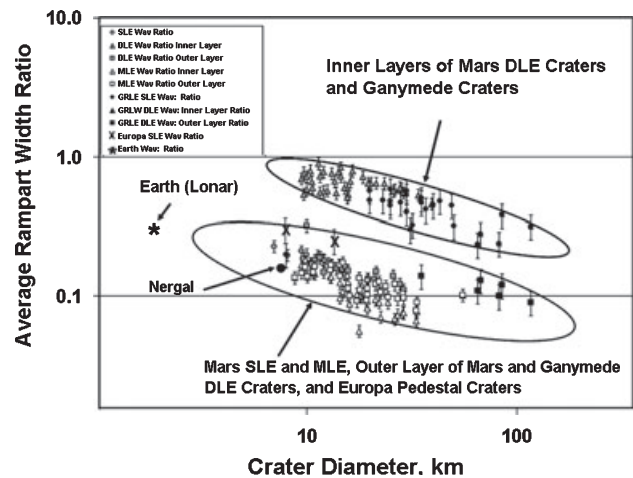

Fig. 6. This plot shows ramparts fall in to two major groups that narrow proportionally relative to the size of their parent crater. This suggests that the process of rampart building is less effective as craters size grows, and ejecta run-out distance increases. Ellipses enclose members of each parameter and are not meant to define limits beyond where data exists.

layer. This measurement adds confidence to our values of W_{av} for DLE inner ejecta layers.

Rampart height would also be a valuable parameter for our analysis. Shadow-length measurements are the most reasonable technique for measuring those heights; the low image resolution for Ganymede and Europa combined with the relatively small vertical relief of the ramparts prevent acquisition of accurate height measurements using shadow data (Bray 2009). However, ejecta ramparts are typically much wider than high (Mouginis-Mark and Garbeil 2007), so their width is a good proxy for their volume. Consequently, we have not measured rampart height for either GRLE or Martian layered ejecta craters.

Rampart Width (W_{av})

We have measured the average width of the distal ramparts of each ejecta layer of the craters in this study because this parameter likely provides information about the rheology of the ejecta during its emplacement. Average width of each ejecta layer's distal rampart likely provides information about rheology of the ejecta during emplacement. We make at least 10 measurements of the rampart width in widely varying locations across the ejecta blanket edge (see discussion on measurement error for details of how rampart edges are located) and take the mean of these measurements to determine average rampart width (W_{av}) ratio by dividing W_{av} by crater radius (similar to calculation of EM).

The average width of ramparts for each crater listed in Tables 1–3 is plotted versus the diameter of that crater in Fig. 5. This plot shows that the width of ramparts of all types of layered ejecta craters increases with crater size. The W_{av} ratio with crater size data plotted in Fig. 6 shows that the relative width of ramparts actually decreases as crater size increases for all types of craters.

These plots show that different types of layered ejecta morphologies, even those from different solar system bodies, cluster into groups with similar rampart width characteristics. For example, ramparts of the inner ejecta layers of GRLE and Martian DLE craters generally have similar widths, for a given crater size, which are systematically wider than ramparts of any other crater types or their layers. By contrast, the ramparts of the outer layers of Martian DLE craters, Martian SLE craters, MLE (all ejecta layers) craters, Europa craters, and Lonar crater are similar and have relatively narrower width. Ganymede's Nergal is an exception, displaying narrower ramparts than those of other GRLE craters. Rampart width of the outer ejecta layer of GRLE craters also appears to be unique as they have values intermediate between the GRLE and Martian DLE inner ejecta layer widths and those of Martian SLE, MLE, and DLE outer layers.

Ejecta Mobility (EM)

We calculated the ejecta mobility (EM) of the ejecta layers of craters in this study in order to investigate what EM implies about conditions that control ejecta emplacement. Previous work suggested that the distance
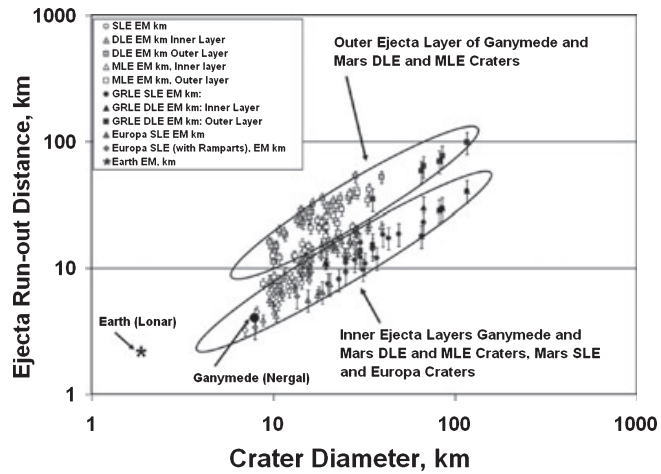
Fig. 7. This diagram shows that ejecta run-out distances of ejecta layers fall into two groups that increase with increasing crater size. Ellipses enclose members of each parameter and are not meant to define limits beyond where data exists.
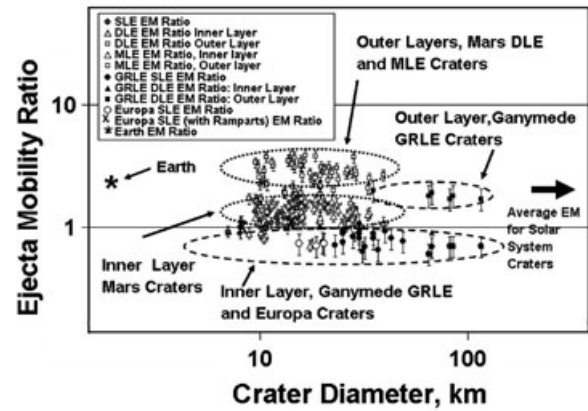

Fig. 8. This diagram shows that while the extent of ejecta layers around all gravity dominated craters are self-similar with crater size, the average EM ratios of ejecta layers of Ganymede and Europa craters are systematically less than those of the same ejecta layers (inner versus outer ejecta layers) of other craters in the solar system. Ellipses (dashed lines) enclose members of each parameter and are not meant to define limits beyond where data exists.

to which ejecta flows across the surface can be influenced by a number of factors, including the fluidity of the ejecta, angle of material ejection from the growing crater, and surface roughness (e.g., see Mouginis-Mark 1978; Kargel 1989; Barlow 1994, 2005b; Neal and Barlow 2003, 2004; Barnouin-Jha et al. 2005). The method we employed to measure EM is somewhat different from previous workers who define ejecta mobility as the maximum distance ejecta have flowed from a parent crater. Instead, we have measured EM as the average run-out distance of the ejecta of each layer by averaging the distance of approximately 10 individual radii (to include as many different azimuths as possible) from the crater rim to the outer edge of the layer (including the smallest and largest run-out distances). Normalizing this value of ejecta extent to parent crater radius produces a dimensionless number we call the average EM ratio. We have adopted this method of measuring EM to enable ready interpretation of the data and avoid difficulties arising from comparison of long run-out ejecta lobes produced by highly oblique impacts with the more common symmetrical ejecta layers produced by steeper angle impacts. Our method also tends to reduce systematically the scatter in EM values for any given crater size.

The average ejecta run-out distance and average EM ratio of craters measured in this study are plotted against crater diameter in Figs. 7 and 8, respectively. Figure 7 shows that the average run-out distance of fluidized ejecta increases with increasing size of the parent crater, no matter the type of crater or on which planet it occurs. However, Fig. 8 also confirms previous

observations by Horner and Greeley (1982), Neal and Barlow (2003, 2004), and Barlow (2005a, 2005b, 2006a, 2006b) that the average ejecta run-out distance is the same relative to the size of the parent crater (i.e., self-similar with crater size), and that the mobility of Ganymede layered ejecta is systematically less than that of Martian layered ejecta for a given type crater. In addition, the average EM ratio of Europa layered ejecta appears to be similar to that of Ganymede and is systematically less than that of ejecta of other planets, as is the average EM value for the pedestal craters on Dione (e.g., 0.8 ± 0.04).

Self-similarity allows the ready calculation and comparison of average EM ratios of ejecta for our test craters with those from other investigations (i.e., Neal and Barlow 2003, 2004; Barlow 2005b; also see Melosh 1989, p. 124), These average EM ratio values for each layer on each type of crater on each body are listed in Table 4, and plotted in Fig. 9. These data indicate that, with the exception of the outer ejecta layer of GRLE craters, there are only minor differences (approximately 9%) between data set. We suggest that this is the result of our measurements of average ejecta run-out distance instead of its maximum ejecta run-out distance used in previous EM calculations. The large difference in EM ratio of the outer ejecta layers of GRLE craters may be due to difficulty in identifying the outer edge of this layer owing to its subtle topography and the low-resolution of most Ganymede images. Recent image processing tools have made identification of this layer easier.

Table 4. Ejecta layer morphometric parameters (i.e., average EM ratios, r, and average Γ) for fluidized ejecta craters with ramparts found on Mars, Ganymede, Europa, and Earth.

Planet and ejecta layer	Average ejecta mobility (EM) ratio, this study	Average ejecta mobility (EM) ratio (from Neal and Barlow 2004; and Barlow 2006a, 2006b)	Rampart widening (i.e., grow) rate (r)	Average ejecta sinuosity Γ
Mars SLE	1.27	1.5	−0.28	1.1
Mars DLE inner layer	1.37	1.5	−0.72	1.09
Mars DLE outer layer	3.17	3.3	−0.68	1.14
Mars MLE inner layer	1.25		−0.32	
Mars MLE outer layer	2.31	2.5	−0.42	1.25
GRLE SLE (Nergal)	1			1.12
GRLE DLE inner layer	0.86	0.9	−0.78	1.1
GRLE DLE outer layer	1.86	1.25	−0.64	1.2
Europa pedestal	0.81			1.1
Earth (Lonar)	2.34			
Average other planets		2.35		
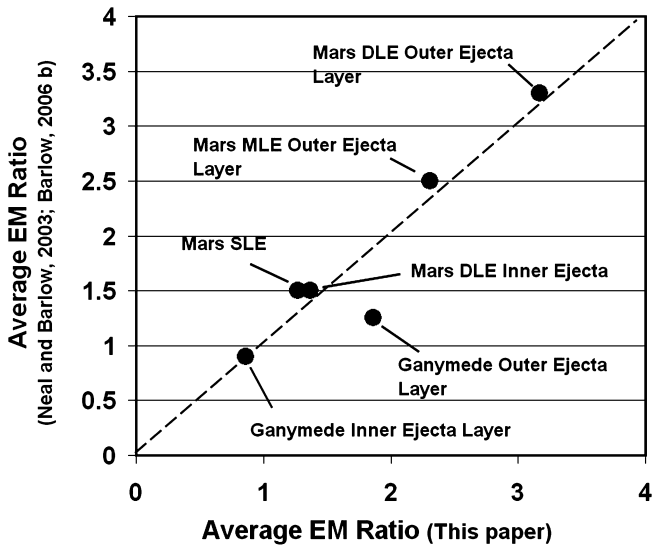
Fig. 9. This diagram shows that there is generally good agreement between our average EM ratio data and those of Neal and Barlow (2003) and Barlow (2006b), except for the outer ejecta layer of Ganymede craters where difficulty in identifying the subtle outer edge of this ejecta layer on the low-resolution images may have affected earlier measurements.

Fig. 10. Average width (in km) of ramparts shows clustering into two major groups that increase with average ejecta run-out distance (in km). Ellipses enclose members of each parameter and are not meant to define limits beyond where data exists.

The Relationship between W_{av} and EM

How rampart dimensions change with the run-out distance can provide useful information about the mechanics of ejecta flow, as well as environmental conditions that influenced flow (see Aranson and Tsimring 2006). Consequently, we consider the relationship between rampart width and ejecta run-out distance (i.e., average EM) in this section.

Figure 10 shows that ramparts of all ejecta layers of each crater type widen with increased run-out distance.

As with data in previous plots, these data form clusters with similar characteristics, e.g., the inner ejecta layers of Martian DLE and GRLE craters form one major group and the other ejecta layers of other types of craters form another.

These major groups consist of data points from the individual ejecta layer of each crater type. We fit a regression line through the data points shown in Fig. 10 and obtain an exponent that describes the rate at which ramparts widen as a function of crater size for each layers type. The exponents cluster into similar groups (Fig. 11) that include (1) the inner ejecta layer of Martian DLE and GRLE craters, (2) the outer ejecta layer of Martian DLE and GRLE craters, and (3) the
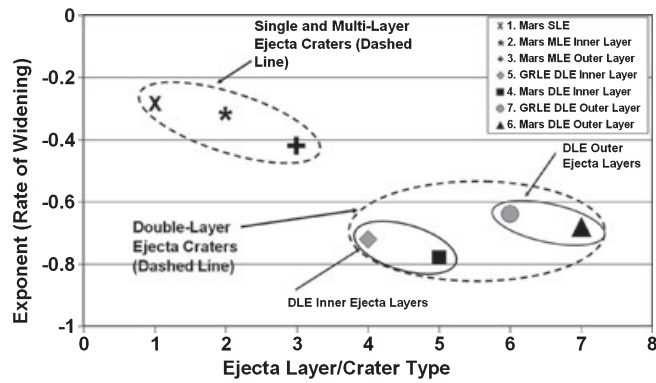
Fig. 11. Rate of widening of ramparts (i.e., the exponent calculated from the regression analysis of the data points of each layered ejecta type listed in Table 4) plotted against the type of layered ejecta crater.
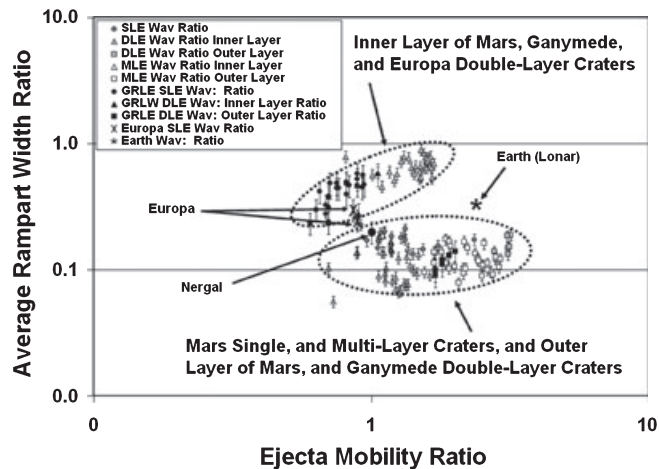

Fig. 12. This plot shows clustering of the data into the same two major groups shown in Fig. 10, suggesting that the ejecta deposits of each crater type are uniquely different from one another. This plot shows that the Ganymede crater Nergal clearly falls with the data points of Martian SLE craters suggesting that Nergal is, indeed, a SLE crater, while the other GRLE craters are DLE craters. The two Europa craters fall between the cluster of the inner ejecta layer of GRLE craters and Martian SLE craters. Ellipses (dashed lines) enclose members of each parameter and are not meant to define limits beyond where data exists.

ejecta layers of Martian MLE and SLE craters. Assignment of the two Europa craters to a group is not warranted due to the small number of data points. These figures suggest that, independent of planet, the rate of widening of ramparts is unique to specific types of layered ejecta craters. This also suggests that there is a fundamental difference in the behavior of the ejecta of different types of craters, and that GRLE and Martian DLE craters may represent the same crater type on different planets.

We take analysis of these data a step further by plotting average EM ratio against the W_{av} ratio in Fig. 12. To a first order, this plot also shows clustering of the data into two major groups. One of these groups includes the ejecta layers of Martian SLE, MLE, the outer ejecta layers of Martian DLE and GRLE craters, and Ganymede's Nergal crater. The other major group includes the inner ejecta layers of Martian DLE and GRLE craters. The presence of these two groups support the earlier suggestion by Horner and Greeley (1982), Neal and Barlow (2003, 2004), and Barlow (2005a, 2005b, 2006a, 2006b) that double-layered ejecta are fundamentally different than other types of layered ejecta, and indicates that the inner ejecta layer is mainly what makes the ejecta of these craters different from other types of layered ejecta craters.

The two Europa rampart craters are only slightly within the boundaries of the group that mainly includes inner ejecta layers. This is too few craters to be sure that Europa craters really belong to this group, are members of an intermediate group, or are scattered data from the other group. Only more data (currently not available from Galileo or Voyager images) can answer this question. In addition, Lonar is the only terrestrial crater representative. It appears to fall outside of either of the major groups. This may be due to the relatively small size of this crater (at the size boundary between gravity and strength dominated sizes of terrestrial craters) that may mean that its EM is controlled by a different scaling factor than the other craters in this study.

Many GRLE craters display no identifiable outer ejecta layers, but the data are consistent with these craters being DLE craters where the outer ejecta layer is missing or unrecognizable. Lack of such identification is not surprising considering the general quality of the available image data.

Sinuosity/Lobateness (Γ)

Neal and Barlow (2003, 2004), Neal (2004), and Barlow (2005b, 2006a, 2006b) measured Γ for Ganymede and Martian layered ejecta craters. Lobateness, like EM, is generally regarded as an indicator of the fluidity of the ejecta resulting from the volatile content in the ejecta and/or the degree of interaction of the ejecta curtain with the atmosphere (Barnouin-Jha and Schultz 1998).

We have relied heavily in this study on the Γ data collected in these previous studies. However, these Γ results are augmented by data we have collected (Table 4) when the sinuosity data did not previously exist for a particular crater type (e.g., Europa craters) or where our preliminary measurements do not agree with previous Γ values.

Previous studies show that Γ varied little with latitude on both Ganymede and Mars (Barlow 2004; Neal 2004). EM varies little with latitude on Ganymede (Neal 2004) but shows a slight increase toward higher latitudes of Mars, which may result from increasing subsurface ice concentration poleward of about 40° latitude on Mars (Barlow 2004, 2006a). These previous studies also found that Γ is nearly constant with crater size on Ganymede but increases slightly with increasing diameter on Mars (Barlow 1994; Neal 2004). We use the Γ values in the Martian midlatitudes from Barlow (2004) in this study.

While our preliminary findings generally agree with previous finding of Neal and Barlow (2003, 2004) for the inner ejecta layer of GRLE craters, we disagree with their value for the outer ejecta layer. Based on our measurement of Γ of the ejecta layers of Achelous crater (see Fig. 4), Γ for the inner ejecta layer is approximately 1.06 and Γ for the outer ejecta layer is approximately 1.20. Moreover, our visual inspections of other GRLE craters suggest that Achelious is not unique among double-layer GRLE craters (see Fig. 1), and that their Γ values are generally comparable with the respective layers of Martian DLE craters. We suggest that differences between our values Γ of the outer ejecta layers of GRLE craters and those of previous studies may be due to the same reasons for the differences between the two EM data sets (see above).

DISCUSSION

The presence of layered ejecta craters on Ganymede and Europa with ejecta lobes that terminate in ramparts, combined with evidence of ground-hugging flow suggests that the ejecta of these craters were fluidized during emplacement, similar to that of Martian layered ejecta. The morphometric and morphologic characteristics of most of the ejecta layers of these craters (see details below) are similar to Martian DLE craters. However, the small Ganymede crater Nergal is different and appears to be the Ganymede equivalent of Martian SLE craters. This supports the proposal of Barlow et al. (2000) that there may be only two fundamental types of layered ejecta craters; i.e., DLE craters and MLE craters, of which SLE craters are an endmember. These two different types may reflect difference in rheology.

The presence of these craters also provides an important test for the two leading models of fluidized ejecta formation. One of these models proposes that atmospheric gases are the fluidizing agent, while the other relies on volatiles (generally water or ice) contained in the target materials for ejecta fluidization.

However, neither Europa nor Ganymede had an appreciable atmosphere throughout their histories and thus the presence of layered ejecta craters on the two bodies suggests that an atmosphere is not required for ejecta fluidization. But, this does not mean that by default the other model (i.e., volatiles in the target materials) is the answer either. This is because impact crater formation on other icy satellites should generate impact-induced liquid water that is mixed in the ejecta. If water were the cause for fluidization, then the ejecta deposits of these craters should exhibit evidence of flow, but instead their ejecta deposits more resemble lunar ejecta. Consequently, while the presence of volatiles in target materials may be necessary for ejecta fluidization, their presence alone does not cause ejecta fluidization even in geologically active bodies such as Titan and Enceladus.

A possible influencing factor on whether ejecta are fluidized may be suggested by the distributions of the different types of layered ejecta craters on each body. For example, GRLE craters are restricted to the grooved terrain of Ganymede and Martian DLE craters are concentrated in the northern lowlands of Mars (e.g., Barlow 2005a; Boyce and Mouginis-Mark 2006). The cause of the correlation with terrain type is unclear. In the case of Ganymede, it could be a result of disruption of flow by topography in the high-relief (on the order of the scale as the observed ramparts), dark, heavily cratered terrain (see Wada and Barnouin-Jha 2006), or difficulty in identification of low-relief features like ramparts in such complex terrain (Horner and Greeley 1982). Alternatively, there may be a genetic relationship between ejecta fluidization and the tectonically active grooved bright terrain, caused by the physical or chemical properties of the target materials (e.g., high concentrations of volatiles or elevated temperature relative to dark terrain, also see Stewart et al. 2008). The presence of layered ejecta craters on Europa would tend to favor this alternative. It is also possible, but unlikely, that their distribution is a statistical effect related to the size of the sample area (Horner and Greeley 1982).

Moreover, the restriction of GRLE craters to only the grooved terrain of Ganymede also provides a test for the hypothesis that the characteristics of the impactor may influence fluidization. A geographically restricted distribution for these craters suggests a nonrandom process (such as cratering), and hence, that the characteristics of impactors have played no role in producing ejecta fluidization.

The rest of this section will be dedicated to the discussion of the morphologic and morphometric observation in the previous section and what they may mean.
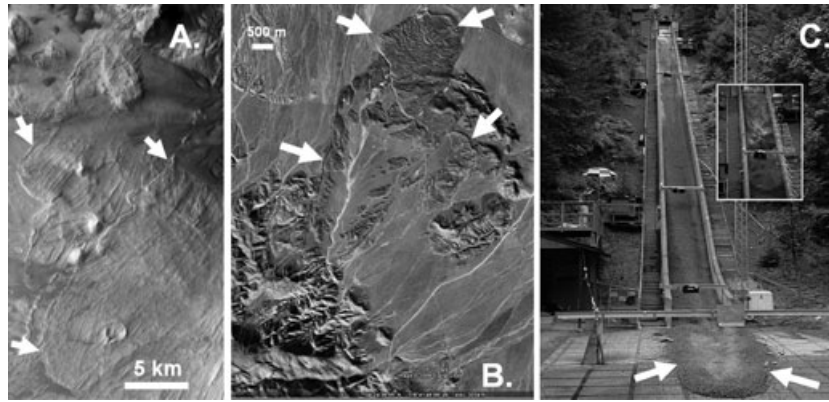
Fig. 13. Ramparts (white arrows) that resemble those of impact ejecta also developed at the margins of natural flow as shown in A) that is a long-run-out landslides in Valles Marineris of Mars (NASA THEMIS VIS images V18800002), B) the Blackhawk landslide, California (Google Earth); and C) an experimental debris flow with coarse grain rampart produced at the U.S. Geological Survey's 93 m Debris Flow Flume (from Matthew and Iverson 2007).

Ramparts

Knowledge of how these features develop is necessary to fully understand what these features reveal about fluidized ejecta emplacement. However, the origin of ejecta ramparts is still controversial (e.g., Schultz 1992; Baloga et al. 2005), but it is clear that these features are primary flow features. We suggest that an approach with great potential for shedding insight into the mechanics of ejecta rampart development is using ramparts in gravity-driven, rapid, flowing particulate materials on Earth as an analog.

Rampart ridges that resemble those of impact ejecta develop at the margins of flowing masses such as debris flows and long run-out landslides (Figs. 13A and 13B), as well as in some laboratory experiments (Fig. 13C) and numerical simulations. These features are generally regarded as indicators of the physical characteristics of the flowing materials, dynamics of the flow, and environment in which they formed (e.g., see Shreve 1966; Savage and Hutter 1989; Iverson 1997; Major and Iverson 1999; Pouliquen and Vallance 1999; McSaveney and Davis 2005; Barnouin-Jha et al. 2005; Wada and Barnouin-Jha 2006; Campbell 2006).

It is tempting to assume that the flow of impact crater ejecta and terrestrial mass movements across the surface are both controlled by the same mechanics because they are both flowing granular masses composed of fragmented debris. However, we suggest that this assumption would ignore an important difference between the initial dynamical conditions of the two flows: i.e., the initial velocity (and energy) distribution of particles in ejecta is nearly the reverse of that of landslides or debris flows.

Ejecta is excavated from the transient crater cavity in a generally systematic fashion in all impact craters. It
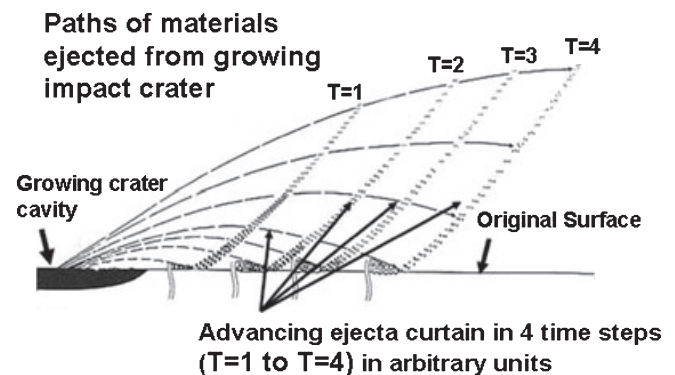

Fig. 14. Sketch of the calculated paths of material ejected from a lunar impact crater showing that it is launched in ballistic trajectories from a developing crater. This relationship between position, time, and ejection velocity produces a cone-shape ejecta curtain that sweeps outward (shown at 4 time steps) (inspired by a figure in Oberbeck et al. 1975).

is excavated progressively outward from the impact point with lower and lower energy and velocity. This orderly process produces a thin ejecta curtain shaped like an inverted cone that sweeps rapidly outward from the crater rim (Gault et al. 1968; Oberbeck 1975; Melosh 1989, p. 74–75, 92) (Fig. 14). When the transport mechanism is purely ballistic, the debris in this curtain travels in ballistic arcs striking the ground first at its base, near the crater rim, then at greater distances with progressively higher velocity. The effect of this orderly process is that ejecta particles have only limited dynamical interactions in flight or on the surface because they land progressively further from their origin and at progressively higher velocity. This inhibits grain-to-grain collisions and hence the transfer of momentum in ballistic ejecta, which is important in granular flow

(e.g., see Savage and Hutter 1989; Iverson 1997; Campbell 2006). By contrast, particles in terrestrial mass movements are driven down-slope by gravity. As a result, particles highest up the slope not only have greatest energy, but they are also able to transfer that energy to particles down slope through collisions. This inability to readily transfer momentum between particles may be a major reason that ejecta deposits on most airless bodies show only limited ejecta flow (Boyce and Mouginis-Mark 2009). Therefore, we suggest that in order for substantial fluidization to occur in ejecta, this orderly process must be disrupted in a way that more closely produces the velocity distribution of particles in gravity-driven mass flows.

A leading hypothesis, and the one we adopt here for the formation of marginal ramparts of granular flows, proposes that these features are the result of flow instability. This instability grows from a high-friction band of coarse particles that accumulates at the propagating flow margins of gravity-driven, thin flows of poorly sorted, wet, or dry cohesionless fragmented debris (e.g., Savage and Hutter 1989; Iverson 1997; Pouliquen and Vallance 1999; Denlinger and Iverson 2001; Iverson and Denlinger 2001). This model has emerged from considerable experimental, field, and numerical modeling studies.

In this model, coarse particles segregate to the surface of the flow by kinetic sieving and are transported by shear to the propagating flow front where the largest particles accumulate to produce a high-friction band. In flows of granular materials (such as ejecta) with particles of substantially different sizes, kinetic sieving occurs when smaller particles move preferentially downward as voids in the moving mass open and close, while proportionally more large particles than small ones are squeezed upward to the free surface (e.g., Middleton 1970; Savage 1987). This process is partly controlled by the strength of the gravity field in which the flow is moving and as a result should tend to be more efficient on planets with high-gravity fields.

Friction between the flow and the rough bed results in minimum velocity at the bed and maximum velocity at the free surface, producing a conveyor belt-like movement within the flow (see Pouliquen and Vallance 1999). This transports large particles that segregate to the surface to the flow front. These large particles accumulate at the flow front if they are too large to be overrun and recirculated back into the flow. Those large particles that accumulate and form a band at the front of the flow are pushed along as it moves forward. As the largest particles in a natural grain flow are commonly more angular than smaller particles, the coarse mixture of grains at the front of
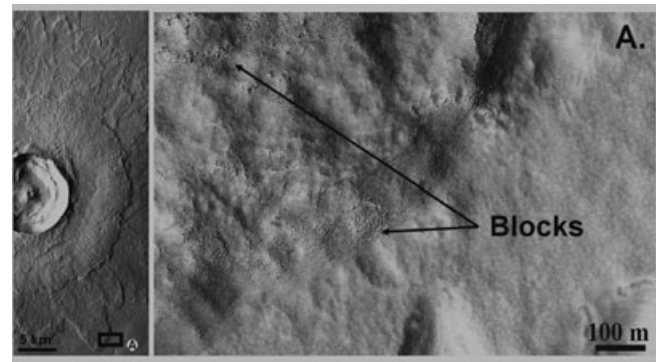

Fig. 15. Abundant blocks on the distal margins (i.e., the rampart) of the outer ejecta layer of the fresh Martian DLE crater Steinhiem are shown in the HiRISE image (Mars Reconnaissance Orbiter HiRISE image PSP-008303-2345) at the right (A). The context image on the left is THEMIS VIS 21149003.

the flow have greater Coulomb friction than the finer grain debris that follow behind (Savage and Hutter 1989; Iverson 1997; Pouliquen and Vallance 1999; Denlinger and Iverson 2001; Iverson and Denlinger 2001). As a result, this band of coarse particles tends to slow the flow and is pushed forward and up into a ridge by the moving body of finer particles behind.

This model predicts that if ejecta behave as flowing granular material during emplacement, then ejecta ramparts should be composed of debris dominated by coarse sizes. Consequently, ejecta ramparts of Ganymede, Europa, and Mars (and the Earth) should be coarse-grained. This appears to be the case, at least on Mars. Barnouin-Jha et al. (2005) reported high block density and relatively high-thermal inertia associated with Martian crater ramparts. We also have observed high concentrations of coarse materials in Martian layered ejecta ramparts in recent high-resolution images (Fig. 15).

This particle size segregation/accumulation mechanism should operate in nearly any environment on solid planetary surfaces to form ramparts, but this process can be affected by other factors (see Aranson and Tsimring 2006). Studies of gravity-driven granular flows have found that the development of ramparts may be affected by the presence of water, particle size distribution, flow velocity, and the strength of the gravity field. We assume that these same factors have similar effects on ejecta flows and development of their ramparts.

Water can have important consequences to rampart development in granular flows. For example, water inhibits kinetic sieving and size segregation, and hence rampart development through buoyancy effects reduces

settling velocity because water lowers the contrast between the densities of particles (Pouliquen and Vallance 1999; Denlinger and Iverson 2001). To a lesser degree, viscous effects also slow downward movement of the particles and retard particle segregation. Consequently, with all other parameters held constant, wet flows should have a reduced supply of coarse particles to deliver to the front of the flows possibly resulting in relatively smaller ramparts compared with those in dry materials. Ganymede and Europa ejecta that most likely contained water due to shock induced melting and vaporization of the icy crust (see Kieffer and Simonds 1980; Stewart et al. 2001, 2004, 2008; Stewart and Ahrens 2005), consequently with all else being equal, their ramparts should be narrower than for dry ejecta. But the width of their ejecta ramparts is similar to those of the same type of craters on other planets (Figs. 5 and 6), suggesting that they either all have included water or that other factors have counterbalanced water's influence on rampart development on these bodies.

One of these factors, and one that could possibly counterbalance the morphologic effects of water, is deflation of the body of the flow by desiccation. Deflation of the body of a wet flow is observed in debris flows, both in nature and in experiments (e.g., Iverson 1997; Major and Iverson 1999; Pouliquen and Vallance 1999; Denlinger and Iverson 2001; Savage and Iverson 2003). This occurs after the flow halts and water seeps out of the water-charged, fine-grain body that develops behind the relatively dry rampart. Observations have shown that this deflation is not uniform, because the coarse-grain rampart contains relatively much less water than the body of the flow. This differential deflation leaves the rampart appearing to be larger and wider than it was during the active flow.

The strength of the gravity field also may be important in rampart development because the equations of motion that govern rampart development include a gravity term. Like water, gravity's effects on different processes that contribute to rampart development may counterbalance. For example, the efficiency of kinetic sieving (and, hence the budget of coarse particles to build the rampart) is controlled by settling velocity, which is directly related to the acceleration of gravity. However, the time for this process to operate is also a function of gravity because ejecta run-out velocity scales inversely with gravity (Melosh 1989, p. 124). This means that for ejecta deposits with the same run-out distance, but on bodies with different gravity fields where the velocity of the flow is different, there is more time for rampart development (and hence more extensive ramparts) on bodies with weaker gravity fields than on stronger ones.

Rampart dimensions also can be affected by the inherent size-frequency distribution of particles in the ejecta. For example, in the particle size segregation/accumulation model, ramparts grow and widen relatively slowly in particulate material containing a paucity of large particles in comparison with those containing significantly more coarse grains. The size-frequency distribution of particles generated by impact into dry rock generally follows a power law relation

$$N(m) = C_f m^{-b} \qquad (3)$$

(where C is a constant, $N(m)$ is the cumulative number of fragments of mass equal to or greater than mass m) with an exponent $-b$ that commonly ranges between 0.8 and 0.9 (Melosh 1989). However, this exponent can be substantially changed by impact into already highly fragmented materials (e.g., loosely cemented clastic sediments) (Nordyke and Williamson 1965) or water-rich targets, which tend to cause greater comminution of rock (Kieffer and Simonds 1980; Wohletz and Sheridan 1983) to produce ejecta deficient in large particles. Hence, either of these possibilities could retard rampart growth and widening resulting in relatively smaller, narrower ramparts for a given size crater.

Experiments and numerical modeling of granular flows suggest that flow velocity also may affect rampart development (Pouliquen and Vallance 1999). As flow velocity increases, granular temperature also generally increases, which diminishes size segregation and causes flow fronts that are more diffuse. As a result of the effects of velocity, ramparts should be largest on planets with the weakest gravity and lowest velocity ejecta, while ramparts of relatively small craters (that produce relatively low-velocity ejecta with shorter ejecta run-out distances) will have proportionally larger and wider ramparts compared with those of larger craters.

The development of ramparts, as with the ejecta run-out distance, also can be affected by the roughness or the erodability of the surface. This is mainly because of frictional effects that slow ejecta over comparatively rough or erodable surfaces, and might add to the slowing power of the course materials at the propagating flow fronts.

While the effects of these factors might collectively cancel in some instances, there may be cases where one factor can dominate rampart size. The data shown in Figs. 5, 6, 10, 11, and 12 indicate that rampart morphometry is different from crater type to crater type and suggests that this may happen. These differences may be the result of differences in rheology of the ejecta of different types of crater caused by one or more of these factors. But determining which ones will require

more extensive modeling and supporting observation, which is beyond the scope of this study.

It should also be mentioned that there are other models for rampart development. An alternative dispersive stress mechanism has been proposed for the development of ramparts by Bagnold (1954) and Vallance (1994), which involves shear-driven, particle size segregation within the flow. In addition, Pierson and Costa (1987), Major and Iverson (1999), and Baloga et al. (2005) have modeled rampart development as an instability produced by friction with the surface at the leading edge of the flow. The model requires shear to mainly occur in a thin zone at the base of the flow in a process called "basal glide" (see Baloga et al. 2005; Barnouin-Jha et al. 2005), but with very little shear within the flow. As a result, transport and accumulation of coarse particles at the propagating flow margins does not occur in these models. However, there is little experimental or theoretical evidence in support of these models (see summary article by Aranson and Tsimring 2006). Schultz (1992) also has proposed that ejecta ramparts form as a result of intense vortices created by the advancing ejecta curtain through the atmosphere, and that ejecta smaller than a certain size become entrained in the ring vortices. He also suggests that larger size particles are carried without suspension and deposited as a terminal rampart. The lack of an atmosphere on Ganymede and Europa put this mechanism in doubt, but an impact-generated gas cloud may have played a role.

Ejecta Mobility

As observed in previous studies (Horner and Greeley 1982; Neal and Barlow 2003, 2004; Barlow 2005b), EM ratio values of the ejecta of GRLE craters indicate that this ejecta scale in a self-similar way with crater size. Remarkably, it was also found that the EM ratios of ejecta layers on Ganymede are systematically less than those of Martian craters, or craters on other solar system bodies of the size that are dominated by gravity (Melosh 1989, p. 124). We have found that this is also true for Europa pedestal craters, whose average EM ratios are similar to that of Ganymede craters, but less than Martian craters (see Fig. 8).

Self-similarity of these ejecta deposits is not particularly surprising (Melosh 1989, p. 124), but the systematically lower values of the average EM ratio for Ganymede and Europa layered ejecta craters is another issue. A number of suggestions have been offered to explain this observation, including the effects of (1) gravity on ejection velocity, (2) ice on the ejection angle, (3) the cold surface conditions on the viscosity of the ejecta flows, and (4) the relatively higher roughness and erodability of the surface.

These differences in average EM ratios are of particular note, but may be explained by considering the first order governing equations that control EM ratio values (i.e., ejection velocity and the ballistic range of ejecta) where the gravity term in the ejection velocity equation and the gravity term in the ballistic range equation terms cancel (hence, the reason for self-similarity of ejecta with crater size). The relationship of ejection velocity v_e and crater radius R for gravity dominated craters is

$$v_e = 0.28(r/R)^{-e}\sqrt{gR} \tag{4}$$

where r is ejection position within a crater, and the exponent $-e$ ranges from approximately 1.9 to 2.4 (Holsapple and Schmitt 1982; Housen et al. 1983; Melosh 1989). This equation indicates that $v_e/\sqrt{gR}$ is constant at a given value of r/R no matter the size of the crater as long as its excavation is gravity dominated. However, the ballistic range of the ejecta is

$$R_b = v^2_e sin2\phi/g \tag{5}$$

(where ϕ is ejection angle), and the ratio of ejecta range to crater radius R_b/R depends only on r/R. This indicates that distance of ejecta run-out from gravity controlled craters is self-similar with crater size, and with all other factors being the same, all gravity controlled craters should produce ejecta that is self-similar in the same way.

We suggest that considering these equations, the data shown in Fig. 8 can most readily be explained by the laboratory and numerical modeling results of Greeley et al. (1980) and Senft and Stewart (2008), which indicate that the ejection angle (ϕ) of impact crater ejecta increases with the amount of ice in target materials. This would cause ejecta from craters on dominantly icy bodies like Ganymede and Europa to have higher angle trajectories than ejecta from a rocky body, such as Mars or Earth. Such high ejection angles cause ejecta to fall closer to the rim of the parent crater, and with relatively lower horizontal velocity, hence reducing the ejecta's run-out distance.

Neal and Barlow (2003, 2004) and Barlow (2005b) also have proposed that the difference between Ganymede and Mars EM ratio values is caused by cold surface conditions on the surface of Ganymede compared with Mars. They suggest that the lower temperature would raise ejecta viscosity by freezing water in the ejecta. Their argument is based on the supposition similar to the model of Wilson and Head (1984) for the stability of water flowing across the surface of an icy satellite. Wilson and Head (1984) and Barlow (2005b) proposed that vapor loss from the

surface would provoke the formation of ice crystals, and that if the water/ice is well mixed by the turbulence in the flow, the main effect will be a progressive increase in viscosity and yield strength of the flow. However, assuming that fluidized ejecta on Ganymede has a similar excavation depth to that on Mars ejecta for a given size crater (approximately 25–100 m for the craters studied) and adopting the numerical approach of Wilson and Head (1984) for the distance traveled by a flow on icy satellites, the estimated travel distances for ejecta layers of GRLE craters in this study before it freezes is over an order of magnitude greater than the observed run-out distances. This suggests that some other phenomena caused the ejecta to halt long before freezing or likely even before the viscosity changed appreciably due to ice crystal formation. This is also consistent with the thermal calculations of Allison and Clifford (1987) of the time it would take for a water flow on Ganymede to completely freeze at its base (12.5 days for a 5 m and 50 days for a 10 m thick flow, respectively). In addition, using the estimates of fluidized ejecta velocity for Martian craters as a starting point (Baloga et al. 2005; Boyce and Mouginis-Mark 2006) and scaling the velocity for the gravity of Ganymede or Europa, the emplacement of Ganymede or Europa ejecta should be complete within a matter of a few minutes to tens of minutes (depending upon crater size, and hence ejecta flow velocity) for the observed crater size range. This is much less time than it would take for an appreciable amount of water in a flowing mass of debris on these bodies to freeze.

The observed difference in EM ratio values from body to body could also be produced by differences in surface properties such as erodability and/or roughness through their frictional effects. For example, rough and/or erodable surfaces should produce relatively larger ramparts and shorter run-out distances for a given size crater. However, there is little evidence for major differences in roughness and erodability of the surfaces of Mars and Ganymede. Large-scale roughness on both bodies is mainly caused by the pre-impact topography, which is mainly controlled by earlier impact craters. The density of impact craters on Ganymede grooved-terrain is similar to that of typical Martian highland plains (see, Smith et al. 1979b; Shoemaker et al. 1982). Furthermore, there is no observational evidence to support Ganymede (or Europa) as being significantly rougher at smaller-scale (e.g., sub-meter scale), or the surface being more erodible than the surface of Mars (Smith et al. 1979a, 1979b; Ostro 1982; Veverka et al. 1986). Consequently, we suggest that roughness on the scale required for disrupting ejecta flow is most likely not the cause of the

differences in either the ejecta run-out distance or the rate of widening of ramparts.

The EM ratio values should change with increased crater diameter and ejecta depth if roughness or erodability were important factors on these bodies. The effects of these surface properties are a function of the ratio of the thickness of the ejecta flow to the scale of relief of the roughness or the disrupted zone in the erodable layer. Consequently, thick flows should be relatively unaffected while thin flows may be substantially affected by surface roughness or an easily eroded surface. Figure 8 shows that the EM ratio values remain nearly constant with crater size on all bodies and for each ejecta layer studied, suggesting that surface roughness or erodability are not different enough from body to body to be major factors in ejecta run-out distance.

The ejecta mobility data also may provide some insight into the origin of multiple ejecta layers. The origin of inner ejecta layers has been a major unresolved problem since the discovery of layered ejecta craters on Mars over 30 yrs ago. They have been attributed to such phenomena as layering in the target materials (Mouginis-Mark 1981; Senft and Stewart 2008), flow separation and deposition of fine-grain ejecta entrained in impact induced atmospheric vortices (see Schultz 1992; Barnouin-Jha et al. 2005), or surging of the ground-hugging flowing ejecta (Wohletz and Sheridan 1983).

If ejecta layering were caused by excavation into subsurface thick layers of materials of substantially different strength properties (e.g., Mouginis-Mark 1981; Senft and Stewart 2008), the ratio between the average EM ratios of the inner and outer ejecta layers should change with crater size (i.e., this hypothesis proposes that the outer layer is initiated at the beginning of excavation and the next layer at the boundary between major subsurface layers). As crater size increases, and the depth of excavation also progressively increases, the ratio between the depth to the subsurface layer and the size of the crater also changes. However, this is not supported by the data of average EM ratio of the inner and outer ejecta layers (Fig. 8) or crater size (see Fig. 11). This is also true in the case of differences in initiation diameter of fluidized ejecta on Mars (Boyce 1979; Kuzmin 1988; Costard 1989), which is suspected to be caused by a subsurface layer (i.e., water/ice-rich rock) that varies in depth from region to region.

Alternatively, Schultz (1992) has proposed in his atmospheric ejecta emplacement model that multiple lobate ejecta flows are the result of fine-grained lithologies where most of the ballistic ejecta is initially entrained in a vortex and flow separation results in successive stages of emplacement. He suggests these

stages over-run each earlier stage, with the finer fraction remaining entrained in the vortex-driven flow regime the longest and achieves the greatest run-out distances, with emplacement similar to matrix-supported debris flows. This explanation is inconsistent with (1) the data in Fig. 8 because it implies that layering should also be a function of the atmospheric density and scale height, and hence ejecta run-out should not be self-similar with crater size, (2) observations using recent high-resolution images that show ejecta blocks occur on the surface of all ejecta layers, and (3) the absence of atmospheres on Ganymede or Europa.

Wohletz and Sheridan (1983) proposed that ejecta layers could be produced by surging in a way similar to that observed in pyroclastic flows, where surging may be caused by the episodic buildup of gases that drive pulses of ash. Major and Iverson (1999), and Denlinger and Iverson (2001) found that surging in debris flows commonly occurs even with a uniform supply of debris, similar to the conditions expected for ejection of material from the growing crater cavity of an impact crater. However, the self-similarity of average EM ratios with crater size of each layer and the constant nature of EM ratio values with crater size between layers suggest that the timing of development of all layers is a function of the mechanics that control ejection of debris from the growing crater cavity and ejecta run-out. The surging mechanism is most consistent with the observation that after an initial rapid thinning of the ejecta deposits of Martian MLE craters, they decrease only gradually in thickness outward even though a series of ramparts may have developed (Mouginis-Mark and Garbeil 2007; and see Fig. 3). This suggests that ejecta layers of these craters do not override one another outward.

A quantitative model for the origin of these features is lacking, but would be valuable to shed light on this important issue. However, such modeling is beyond the scope of this study and will be addressed elsewhere.

Sinuosity/Lobateness

The cause of lobateness of fluidized ejecta blankets, although still controversial, is generally agreed to be an indicator of the fluidity of the ejecta, and that it is either controlled by the volatile content in the ejecta (e.g., Kargel 1989; Barlow 1994, 2005b) and/or the degree of interaction of the ejecta curtain with the atmosphere (e.g., Barnouin-Jha and Schultz 1998; Suzuki et al. 2007). Barnouin-Jha and Schultz (1998) and Suzuki et al. (2007) amplified on the atmosphere interaction possibility and showed that the advancing ejecta curtain could produce a vortex-ring in the atmosphere that develops instabilities resulting in waves
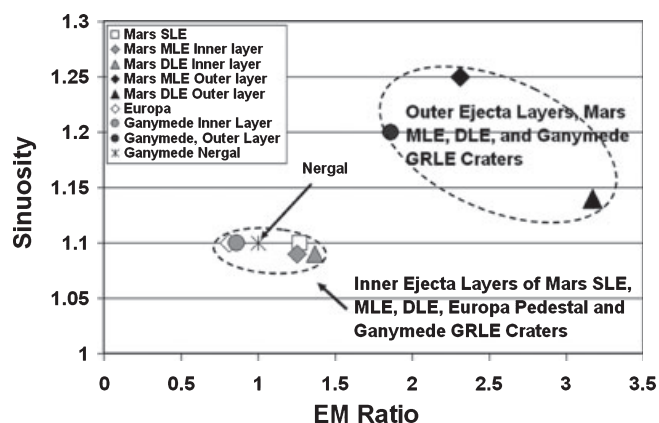

Fig. 16. This plot shows that the ejecta of the different types of craters fall into two major groups defined by their Γ and average EM ratio.

that cause the sinuosity. While this explanation is plausible for Mars, it is not directly applicable to Ganymede or Europa where essentially there was no atmosphere at the present time nor is there evidence for any atmosphere on either body (e.g., Smith et al. 1979a, 1979b). However, this does not preclude such fluidization from being produced by a transient atmosphere generated by impact into and vaporization of volatile-rich targets, providing the gas produced expends outward faster than the ejecta.

A comparison of average Γ and EM ratio values for Ganymede, Europa, and Martian layered ejecta confirms and extends the previous observations of Neal (2004) and Barlow (1994, 2004, 2006a, 2006b) that the ejecta layers with the highest average EM ratios are also the most sinuous (Fig. 16). This most likely indicates differences in the fluidity of materials that make up the different layers with the inner ejecta layers composed of materials with less fluidity than the other ejecta layers. However, it may also be simply that the development of ejecta lobes is a function of run-out distance.

Implications to Fluidized Ejecta Models

None of the simple models for ejecta fluidization entirely fits the observed data at this point. For example, the mere existence of GRLE craters on Ganymede and pedestal craters on Europa suggests that an atmosphere is not required for ejecta fluidization. But these craters do not rule out the possibility that a shock produced transient gas cloud could be important to ejecta fluidization (Schultz 1992; Barnouin-Jha and Schultz 1996, 1998; Barnouin-Jha et al. 1999).

The putative absence of fluidized ejecta on other ice-rich solar system bodies, even those that show geologic activity such as Enceladus, suggests that the presence of abundant volatiles in the target also may not be the sole

cause of ejecta fluidization. Other factors may be involved such as a genetic relationship between ejecta fluidization and the physical or chemical properties of the target materials (e.g., high concentrations of volatiles, relatively elevated subsurface temperature, unique geometry to subsurface layering). More data will be required to shed additional data on this topic.

Most models of ejecta fluidization require some form of volatiles as a fluidizing medium, but a dry granular flow model has been proposed (Wada and Barnouin-Jha 2006). This mechanism could produce the morphologic features observed on GRLE and Europa pedestal craters (i.e., ramparts, lobate distal edges), but there is reason to expect that, at least, parts of the ejecta of these craters should contain substantial amounts of entrained shock generated water (Kieffer and Simonds 1980; Stewart et al. 2001, 2004, 2008; Stewart and Ahrens 2005). Consequently, GRLE and Europa ejecta should initially contain water, making it difficult to make a convincing case for strictly dry granular flow as the primary fluidization mechanism, although the role this water plays in fluidization of the ejecta of these craters cannot be demonstrated conclusively.

CONCLUSIONS

We have identified layered (fluidized) ejecta craters on Ganymede and Europa whose layers terminate in ramparts similar to those of layered ejecta craters on Mars (and Earth). Our analysis of these craters suggests:

1. Together with other morphologic indicators (e.g., lobate, multilayers geometry, and evidence of ground-hugging flow) the ramparts suggest that the ejecta of these craters were fluidized during emplacement, similar to that of Martian layered ejecta.
2. The presence of these craters provides a test for models of ejecta fluidization. However, none of the simple models for ejecta fluidization that require either an atmosphere or water in the target materials alone entirely fit the observation data.
3. The morphology and morphometry of the ejecta of these craters most resembles Martian DLE craters, with the exception of the small Ganymede crater, Nergal, which is a SLE crater. This supports the proposal of Barlow et al. (2000) that there may be only two fundamental types of layered ejecta craters (i.e., DLE craters and MLE craters, of which SLE craters are an endmember) whose differences in morphology may reflect a difference in the rheology of their ejecta.

4. Similar to ejecta deposits on other planets, the extent (i.e., ejecta mobility ratio) of the ejecta layers of Ganymede GRLE and Europa pedestal craters appears to be self-similar. However, they are systematically less extensive, which may be due to increased ejection angles produced as a result of the abundant ice in the target materials.
5. The restriction of Ganymede GRLE craters to the grooved terrain, and the concentration of DLE craters on Mars to the northern lowlands suggests that these terrains may share key characteristics (e.g., high concentrations of volatiles, near surface layering, elevated subsurface temperature) that control the development of the ejecta around these craters.

In addition to these conclusions, this study suggests future lines of investigation critical to understanding ejecta fluidization, specifically 1) laboratory and numerical experiments of flowing multigrain-size granular masses that have the same initial velocity (energy) distribution throughout as does ejecta, 2) development of models of ejecta flow based on the results of these investigations, 3) detailed measurements of the morphologic elements, such as rampart volume, ejecta volume, the radial grooves and longitudinal waves of ejecta deposits of each type of Martian layered ejecta crater to be used as a basis for testing the different models of ejecta flow, and 4) continued detailed investigation of terrestrial impact crater ejecta in order to search for markers that indicate the flow mechanisms which also can be used as a basis to test models of ejecta flow elsewhere in the solar system.

Editorial Handling—Dr. G. R. Osinski

REFERENCES

Alexopoulos J. S. and McKinnon W. B. 1994. Large impact craters and basins on Venus, with implications for ring mechanics on the terrestrial planets. In *Large meteorite impacts and planetary evolution*, edited by Dressler B. O., Grieve R. A. F., and Sharpton V. L. GSA Special Paper 293. Boulder, Colorado: Geological Society of America. pp. 29–50.

Allison M. L. and Clifford S. M. 1987. Ice-covered water volcanism on Ganymede. *Journal of Geophysical Research* 92:7865–7876.

Aranson I. and Tsimring T. 2006. Patterns and collective behavior in granular media: Theoretical concepts. *Reviews of Modern Physics* 78:641–687.

Bagnold R. A. 1954. Experiments on a gravity-free dispersion of large solid spheres in a Newtonian fluid under shear. *Proceedings of the Royal Society of London Series A* 225:49–63.

Baloga S. M. and Bruno B. 2005. Origin of transverse ridges on the surface of catastrophic mass flow deposits on the Earth and Mars. *Journal of Geophysical Research* 110, doi:10.1029/2004JE002381.

Baloga S., Fagents S. A., and Mouginis-Mark P. J. 2005. Formation of the distal ramparts around Martian impact craters. *Journal of Geophysical Research* 110, doi:10.1029/2004JE002338.

Baratoux D., Mangold N., Pinet P., and Costard F. 2005. Properties of lobate ejecta in Syrtis Major, Mars: Implications for the mechanisms of formation. *Journal of Geophysical Research* 110: Art. No. E04011 APR 23.

Barlow N. G. 1994. Sinuosity of Martian rampart ejecta deposits. *Journal of Geophysical Research* 99:10,927–10,935.

Barlow N. G. 2004. Martian subsurface volatiles concentrations as a function of time: Clues from layered ejecta craters. *Geophysical Research Letters* 31, doi:10.1029/2003GRL19025.

Barlow N. G. 2005a. A review of Martian rampart crater ejecta structures and their implications for target properties. GSA Special Paper 384. Boulder, Colorado: Geological Society of America. pp. 433–442.

Barlow N. G. 2005b. Comparison of impact crater morphologies on Mars and Ganymede (abstract #0806). 9th Mars Crater Consortium Meeting.

Barlow N. G. 2006a. Impact craters in the northern hemisphere of Mars: Layered ejecta and central pit characteristics. *Meteoritics & Planetary Science* 41:1425–1436.

Barlow N. G. 2006b. Catalog of large Martian impact craters, version 2.0 (abstract #1337). 37th Lunar and Planetary Science Conference. CD-ROM.

Barlow N. G., Boyce J. M., Costard F. M., Craddock R. A., Garvin J. B., Sakimoto S. E. H., Kuzmin R. O., Roddy D. J., and Soderblom L. A. 2000. Standardization the nomenclature of Martian impact crater ejecta morphology. *Journal of Geophysical Research* 105:26733–26738.

Barnouin-Jha O. S. and Schultz P. H. 1996. Ejecta entrainment by impact generated ring-vortices: Theory and experiments. *Journal of Geophysical Research* 101:21099–21115.

Barnouin-Jha O. S. and Schultz P. H. 1998. Lobateness of impact ejecta deposits from atmospheric interactions. *Journal of Geophysical Research* 103:25739–25756.

Barnouin-Jha O. S., Schultz P. H., and Lever J. H. 1999. Investigating the interactions between an atmosphere and an ejecta curtain. 2. Numerical experiments. *Journal of Geophysical Research* 104:27,117–27,131.

Barnouin-Jha O. S., Baloga S. L., and Glaze L. 2005. Comparing landslides to fluidized crater ejecta on Mars. *Journal of Geophysical Research* 103, doi:10.1029/2003JE002214.

Boyce J. M. 1979. A method for measuring heat flow in the Martian crust using impact crater morphology. Reports of the Planetary Geology Program 1978-1979, NASA Technical Memo 80339, 114–118.

Boyce J. M. and Mouginis-Mark P. J. 2006. Martian craters viewed by the THEMIS instrument: Double-layered craters. *Journal of Geophysical Research* 111 (E10), doi:10.1029/2005JE2638.

Boyce J. M. and Mouginis-Mark P. J. 2008. Preliminary assessment of the morphometry of Martian impact crater ejecta deposit and their implication (abstract #1002). 11th Mars Crater Consortium Meeting.

Boyce J. M. and Mouginis-Mark P. J. 2009. Martian imapct crater ejecta run-out efficiency: Its implications for water in the subsurface (abstract #1337). 37th Lunar and Planetary Science Conference. CD-ROM.

Bray V. 2009. *Impact crater formation on icy Galilean satellites*. Ph.D. thesis, Imperial College, London, UK.

Campbell C. 2006. Granular material flows—An overview. *Powder Technology* 162:208–229.

Carr M. H., Crumpler L. S., Cutts J. A., Greeley R., Guest J. E., and Masursky H. 1977. Martian impact craters and emplacement of ejecta by surface flow. *Journal of Geophysical Research* 82:4055–4065.

Costard F. M. 1989. The spatial distribution of volatiles in the Martian hydrolithosphere. *Earth, Moon, and Planets* 45:265–290.

Denlinger R. P., and Iverson R. M. 2001. Flow of variably fluidized granular masses across three-dimensional terrain 2. Numerical predictions and experimental tests. *Journal of Geophysical Research* 106:553–566.

Elachi C., Wall S., Janssen M., Stofan E., Lopes R., Kirk R., Lorenz R., Lunine J., Paganelli F., Soderblom L., Wood C., Wye L., Zebker H., Anderson Y., Ostro S., Allison M., Boehmer R., Callahan P., Encrenaz P., Flamini E., Francescetti G., Gim Y., Hamilton G., Hensley S., Johnson W., Kelleher K., Muhleman D., Picardi G., Posa F., Roth L., Seu R., Shaffer S., Stiles B., Vetrella S., and West R. 2006. Titan radar mapper observations from Cassini's T3 fly-by. *Nature* 441, doi: 1038/nature04786.

Gault D. and Greeley R. 1978. Exploratory experiments of impact craters formed in viscous-liquid targets: Analogs for Martian rampart craters? *Icarus* 34:486–495.

Gault D. E., Quaide W. L., and Oberbeck V. 1968. Impact cratering mechanics and structures. In *Shock metamorphism of natural material*, edited by French B. and Short N. M. Baltimore, MD: Mono Press. pp. 87–100.

Greeley R., Fink J., Gault D. E., Snyder D. B., Guest J. E., and Schultz P. H. 1980. Impact cratering in viscous targets: Laboratory experiments. Proceedings, 11th Lunar Planetary Science Conference. pp. 2075–2097.

Hack J. T. 1960. Interpretation of erosional topography in humid temperate regions. *American Journal of Science* 258-A:80–97.

Herrick R., Sharpton V., Malin M., Lyons S., and Feely K. 1997. Morphology and morphometry of impact craters. In *Venus II*, edited by Bougher S. W., Hunten D. M., and Phillips R. J. Tucson, AZ: The University of Arizona Press. pp. 1015–1046.

Holsapple K. and Schmitt R. 1982. On the scaling of crater dimensions 2. *Journal of Geophysical Research* 87:1849–1870.

Horner V. and Greeley R. 1982. Pedestal craters on Ganymede. *Icarus* 51:549–562.

Hörz F., Ostertag R., and Rainey D. 1983. Bunte Breccia of the Ries: Continuous deposits of large impact craters. *Reviews of Geophysics and Space Physics* 21:1667–1725.

Housen K., Schmitt R., and Holsapple K. 1983. Crater ejecta scaling laws: Fundamental forms based on dimensional analysis. *Journal of Geophysical Research* 88:2485–2499.

Iverson R. M. 1997. The physics of debris flows. *Reviews of Geophysics* 35:245–296.

Iverson R. M. and Denlinger R. P. 2001. Flow of variably fluidized granular masses across three-dimensional terrain 1. Coulomb mixture theory. *Journal of Geophysical Research* 106 B1:537–552.

Jaumann R., Clark R. N., Nimmo F., Hendrix A. R., Buratti B. J., Denk T., Moore J. M., Schenk P. M., Ostro S. J., and Srama R. 2009. Icy satellites: Geological evolution and surface processes. In *Saturn from Cassini-Huygens*, edited by Dougherty M. K., Esposito L. W., and Krimigis S. M. New York: Springer. pp. 637–681.

Kargel J. S. 1989. First and second order equatorial symmetry of Martian rampart crater ejecta morphologies (abstract). 4th International Conference on Mars. Tucson, AZ: The University of Arizona. 132–133.

Kenkman T., and Schonian F. 2005. Impact craters on Mars and Earth: Implications by analogy (abstract). Workshop on the Role of Volatiles and Atmospheres on Martian Impact Craters. LPI Contribution 1273. Houston, Texas: Lunar and Planetary Institute. pp. 57–58.

Kieffer S. W. and Simonds C. H. 1980. The role of volatiles and lithology in the impact cratering process. *Reviews of Geophysics and Space Physics* 18:143–181.

Komatsu G., Ori G. G., DiLorenzo S., Rossi A. P., and Neukum G. 2007. Combinations of processes responsible for Martian impact crater "layered structures" emplacement. *Journal of Geophysical Research* 112, doi:10.1029/2006JE002787.

Kuzmin R., Bobina N., Zabalueva E., and Shashkina V. 1988. Structural inhomogeneities of the Martian cryosphere. *Solar System Research* 22:121–133.

Lucchitta B. K. 1980. Grooved terrain on Ganymede. *Icarus* 44:481–501.

Major J. J. and Iverson R. M. 1999. Debris-flow deposition: Effects of pore-fluid pressure and friction concentrated at flow margins. *Geological Society of America Bulletin* 111:1424–1434.

Maloof A. C., Stewart S., Weiss B., Soule S., Swanson-Hysell N., Louzada K., Garrick I., and Poussart P. 2009. Geology of Lonar Crater. *Geological Society of America Bulletin* 122, doi:10.1130/B26474.1.

Matthew L. and Iverson R. M. 2007. Revised 2009. Video documentation of experiments at USGS debris-flow flume 1992–2006 (amended to include 2007–2009). U. S. Geological Survey Open-File Report 2007-1315 v 1.1.

McSaveney M. J., and Davis T. 2005. Making grain-bridge connection between two rocky planets (abstract). Workshop on the Role of Volatiles and Atmospheres on Martian Impact Craters. LPI Contribution 1273. Houston, Texas: Lunar and Planetary Institute. pp. 73–74.

Melosh H. J. 1989. *Impact cratering: A geologic process*. New York: Oxford University Press. 245 p.

Middleton G. 1970. Experimental studies related to the problems of flysh sedimentation. Geological Association of Canada Special Paper 7. pp. 254–272.

Moore J. M., Asphaug E., Sullivan R. J., Klemaszewski J. E., Bender K. C., Greeley R., Geissler P. E., McEwen A. S., Turtle E. P., Phillips C. B., Tufts B. R., Head III J. W., Pappalardo R. T., Jones K. B., Chapman C. R., Belton M. J. S., Kirk R. L., and Morrison D. 1998. Large impact features on Europa: Results of the Galileo nominal mission. *Icarus* 135:127–145.

Moore; J. M., Asphaug E., Belton M. J. S., Bierhaus B., Breneman H. H., Brooks S. M., Chapman C. R., Chuang F. C., Collins G. C., Giese B., Greeley R., Head III J. W., Kadel S., Klaasen K. P., Klemaszewski J. E., Magee K. P., Moreau J., Morrison D., Neukum G., Pappalardo R. T., Phillips C. B., Schenk P. M., Senske D. A., Sullivan R. J., Turtle E. P., and Williams K. K. 2001. Impact features on Europa: Results of the Galileo Europa Mission (GEM). *Icarus* 151:93–111.

Moore J. M., Schenk P., Bruesch L., Asphaug E., and McKinnon W. 2004. Large impact features on Europa: Results of the Galileo nominal mission. *Icarus* 171:424–443.

Mouginis-Mark P. J. 1978. Morphology of Martian rampart craters. *Nature* 272:870–872.

Mouginis-Mark P. J. 1979. Martian fluidized ejecta morphology: Variations with crater size, latitude, and target materials. *Journal of Geophysical Research* 84:8011–8022.

Mouginis-Mark P. J. 1981. Ejecta emplacement and the modes of formation of Martian fluidized ejecta craters. *Icarus* 45:60–76.

Mouginis-Mark P. J. and Garbeil H. 2007. Crater geometry and ejecta thickness of the Martian impact crater Tooting. *Meteoritics & Planetary Science* 42:1615–1625.

Neal J. E. 2004. Comparison study of layered ejecta morphologies surrounding impact craters on Ganymede and Mars. M.S. thesis, Northern Arizona University, Flagstaff, Arizona, USA.

Neal J. E. and Barlow N. G. 2003. Comparison study of layered ejecta morphologies surrounding craters on Ganymede and Mars. Large Meteorite Impact Conference. LPI Contribution 4021. Houston, Texas: Lunar and Planetary Institute.

Neal J. E. and Barlow N. G. 2004. Layered ejecta craters on Ganymede: Comparisons with Martian analogs (abstract #1337). 37th Lunar and Planetary Science. CD-ROM.

Nordyke M. D. and Williamson M. M. 1965. The Sedan event, nuclear explosions—Peaceful applications. *PNE*-242F, T10-4500, 43 Edition, U.S. Army Corps of Engineers: 103.

Oberbeck V. R. 1975. The role of ballistic erosion and sedimentation in lunar stratigraphy. *Reviews of Geophysics and Space Physics* 13:337–362.

Oberbeck V. R., Morrison R. H., and Horz F. 1975. Transport and emplacement of craters and basin deposits. *Earth, Moon, and Planets* 13:9–26.

Osinski G. R. 2006. Effects of volatiles and target lithology on the generation and emplacement of crater-fill and ejecta deposits on Mars. *Meteoritics & Planetary Science* 41:1571–1586.

Osinski G., Greive T., and Spray J. 1987. The nature of the groundmass of surficial suevite from the Ries impact structure, Germany, and constraints on its origin. *Science* 1:9–43.

Ostro S. J. 1982. Radar properties of Europa, Ganymede, and Callisto. In *Satellites of Jupiter*, edited by Morrison D. Tucson: The University of Arizona Press. pp. 213–236.

Pierson T. and Costa J. 1987. A rheological classification of subaerial sediment-water flows. *Geological Society of America Reviews in Engineering Geology* 7:1–12.

Pike R. J. 1980. Geometric interpretation of lunar craters. U.S. Geological Survey Professional Paper 1046-C. U.S. Geological Survey, Washington, D.C.

Pike R. J. 1988. Geomorphology of impact craters on Mercury. In *Mercury*, edited by Vilas F., Chapman C., and Mathews M. Tucson, AZ: The University of Arizona Press. pp. 165–273.

Pohl J., Stöffler D., Hall H., and Ernston K. 1977. The Ries crater. In *Impact and explosion cratering*, edited by Roddy D. J., Pepin R. O., and Merrill R. B. New York: Pergamon Press. pp. 343–404.

Pouliquen O. and Vallance J. W. 1999. Segregation induced instabilities of granular fronts. *Chaos* 9:621–630.

Ritter D., Kochel C., and Miller J. 2002. *Process geomorphology*, 4th ed. New York: McGraw-Hill, 560 p.

Savage S. B. 1987. Interparticle percolation and segregation in granular materials: A review. In *Developments in engineering mechanics*, edited by Selvadurai A. P. S. New York: Elsevier Press. pp. 347–363.

Savage S. B. and Hutter K. 1989. The motion of a finite mass of granular material down a rough incline. *Journal of Fluid Mechanics* 199:177–215.

Savage S. B. and Iverson R. 2003. Surge dynamics coupled to pore-pressure evolution in debris flows. In *Debris-flow hazards mitigation: Mechanics, prediction, and assessment*, edited by Richenmann D. and Chen C.-L. Rotterdam: Mill Press 1. pp. 503–514.

Schenk P. 1991. Ganymede and Callisto: Complex crater formation and planetary crust. *Journal of Geophysical Research* 96:15635–15664.

Schultz P. H. 1992. Atmospheric effects on ejecta emplacement. *Journal of Geophysical Research* 97:11623–11662.

Schultz P. and Gault D. 1979. Atmospheric effects on Martian ejecta emplacement. *Journal of Geophysical Research* 84:7669–7687.

Senft L. E. and Stewart S. T. 2008. Impact crater formation in icy layered terrain on Mars. *Meteoritics & Planetary Science* 43:1993–2013.

Shinbrot T., Duong N., Kwan L., and Alvarez M. 2004. Dry granular flows can generate surface features resembling those seen in Martian gullies. *Proceedings of the National Academy of Science* 101:8542–8546.

Shoemaker E. M., Lucchitta B., Wilhelms D., Plescia J., and Squyres S. 1982. The geology of Ganymede. In *Satellites of Jupiter*, edited by Morrison D. Tucson, AZ: The University of Arizona Press. pp. 435–520.

Shreve R. L. 1966. Sherman landslide, Alaska. *Science* 154:1639–1643.

Smith B. A., Soderblom L. A., Johnson T. V., Ingersoll A. P., Collins S. A., Shoemaker E. M., Hunt G. E., Masursky H., Carr M. H., Davies M. E., Cook II A. F., Boyce J., Danielson G. E., Owen T., Sagan C., Beebe R. F., Veverka J., Strom R. G., McCauley J. F., Morrison D., Briggs G. A., and Suomi V. E. 1979a. The Jupiter system through the eyes of Voyager 1. *Science* 204:951–972.

Smith B. A., Soderblom L. A., Beebe R., Boyce J., Briggs G., Carr M., Collins S. A., Cook II A. F., Danielson G. E., Davies M. E., Hunt G. E., Ingersoll A., Johnson T. V., Masursky H., McCauley J., Morrison D., Owen T., Sagan C., Shoemaker E. M., Strom R., Suomi V. E., and Veverka J. 1979b. The Galilean satellites and Jupiter: Voyager 2 imaging science results. *Science* 206:927.

Stewart S. T. and Ahrens T. 2005. Shock properties of H_2O ice. *Journal of Geophysical Research*, 110. doi:10.1029/2004JE002305.

Stewart S. T., O'Keefe J., and Ahrens T. 2001. The relation between rampart crater morphologies and the amount of subsurface ice (abstract #2092). 32nd Lunar and Planetary Science Conference. CD-ROM.

Stewart S. T., Ahrens T., and O'Keefe J. 2004. Impact processes and redistribution of near-surface water ice on Mars. In: *Shock compression of condensed matter-2003*, edited by Furnish M., Gupta Y., and Forbes J., Melville, NY: American Institute of Physics. pp. 1484–1487.

Stewart S. T., Seifter A., and Obst A. W. 2008. Shocked H_2O ice: Thermal emission measurements and the criteria for phase changes during impact events. *Geophysical Research Letters* 35:L23203. doi:10.1029/2008GL035947.

Strom R. G., Wornow A., and Gurnis M. 1981. Crater populations on Ganymede and Callisto. *Journal of Geophysical Research* 86:8659–8674.

Suzuki A., Kumagai Y., Nagata Y., Kurita K., and Barnouin-Jha O. 2007. Modes of ejecta emplacement at Martian craters from laboratory experiments of an expanding vortex ring interacting with a particle layer. *Geophysical Research Letters* 34, L05203, doi:10:1029/2006GL028372, 5.

Vallance J. W. 1994. Experimental and field studies related to the behavior of granular mass flows and the characteristics of their deposits. Ph.D. thesis, Michigan Technical University, Houghton, Michigan, USA.

Veverka J., Thomas P., Johnson T. V., Matson D. K., and Housen K. 1986. The physical characteristics of satellite surfaces. In *Satellite*, edited by Burns J. and Mathews M. Tucson, AZ: The University of Arizona. pp. 342–402.

Wada K. and Barnouin-Jha O. S. 2006. The formation of fluidized ejecta on Mars by granular flow. *Meteoritics & Planetary Science* 41:1551–1569.

Wilson L. 1968. Morphogenetic classification. In *Encyclopedia of geomorphology*, edited by Fairbridge R. W. New York: Routledge. pp. 717–728.

Wilson L., and Head J. W. 1984. Aspects of water eruption on icy satellites (abstract). 15th Lunar and Planetary Science Conference. pp. 924–925.

Wohletz K. H. and Sheridan M. F. 1983. Martian rampart crater ejecta: Experiments and analysis of melt-water interactions. *Icarus* 56:15–37.